Project Number: JDV 0801

Liquid Piston Gas Compression

A Major Qualifying Project Report: submitted to the Faculty of

WORCESTER POLYTECHNIC INSTITUTE

in partial fulfillment of the requirements for the

Degree of Bachelor of Science

By

Cecil Piya _____

Indraneel Sircar _____

Date: February 3, 2009

Approved: _____

Advisor: Professor James Van de Ven

Approved: _____

Co - Advisor: Professor David Olinger

Abstract

The project investigates the use of a liquid-piston to optimize the efficiency of gas compression. Literature review was conducted to understand the thermal-fluids and heat-transfer processes associated with the liquid-piston, followed by the development of a numerical model on Matlab of a liquid-piston compressor. The model was utilized towards modifying properties for enhancing the heat-transfer within the system. The scope of this project included identifying the optimal operating characteristics of the liquid-piston compressor and establishing a foundation for future research.

Table of Contents

Introduction

The global energy crisis and the environmental damage caused by our inordinate dependence on fossil fuels have led us to re-investigate many existing technologies in order to improve their efficiencies and reduce pollution production. Gas compression, a process that is widely utilized in the consumer and the industrial markets, is one such of such technologies that can be significantly enhanced so that it consumes lower amounts of energy during operation and potentially becomes more reliable in terms of providing consistent and optimal outputs. The Liquid Piston Gas Compression project discussed in this report investigates into a novel approach towards improving the compression efficiency of conventional gas compression technologies. As indicated by its name, this project suggests that the solid piston used in conventional gas compression technologies be replaced by a liquid piston. The main goal of such modification is to maximize the extraction of heat energy from the working gas during its compression in order to reduce the input power required for performing the compression.

In this project, a typical gas compression cylinder where the working gas is mechanically compressed is selected for analysis. It basically comprises of a hollow metallic cylindrical chamber where the working gas is brought in through an inlet valve and compressed by the inward motion of a piston oscillating axially inside the chamber. The piston utilized in the analysis is a liquid that maintains a constant volume and temperature. For analytical purposes the volume of the liquid piston is divided into a large number of secondary volumes, each oscillating inside a slender cylindrical bore. The resulting structure is analogous to a honey-combed cylinder as illustrated in Figure 1. This structure facilitates exposure of a larger cylinder surface area to the working gas in order to abet heat transfer. A cam and follower system with a predefined kinematic profile is utilized to drive the oscillatory motions of the liquid piston. During the compression strokes of the system operation, the liquid volumes in each bore travel across the bore length, compressing the gas while also absorbing heat energy in the surrounding bore walls. Once a specified gas pressure ratio of 9.8 is achieved, an outlet valve is forced open to allow the gas to be collected in an accumulator at constant pressure.

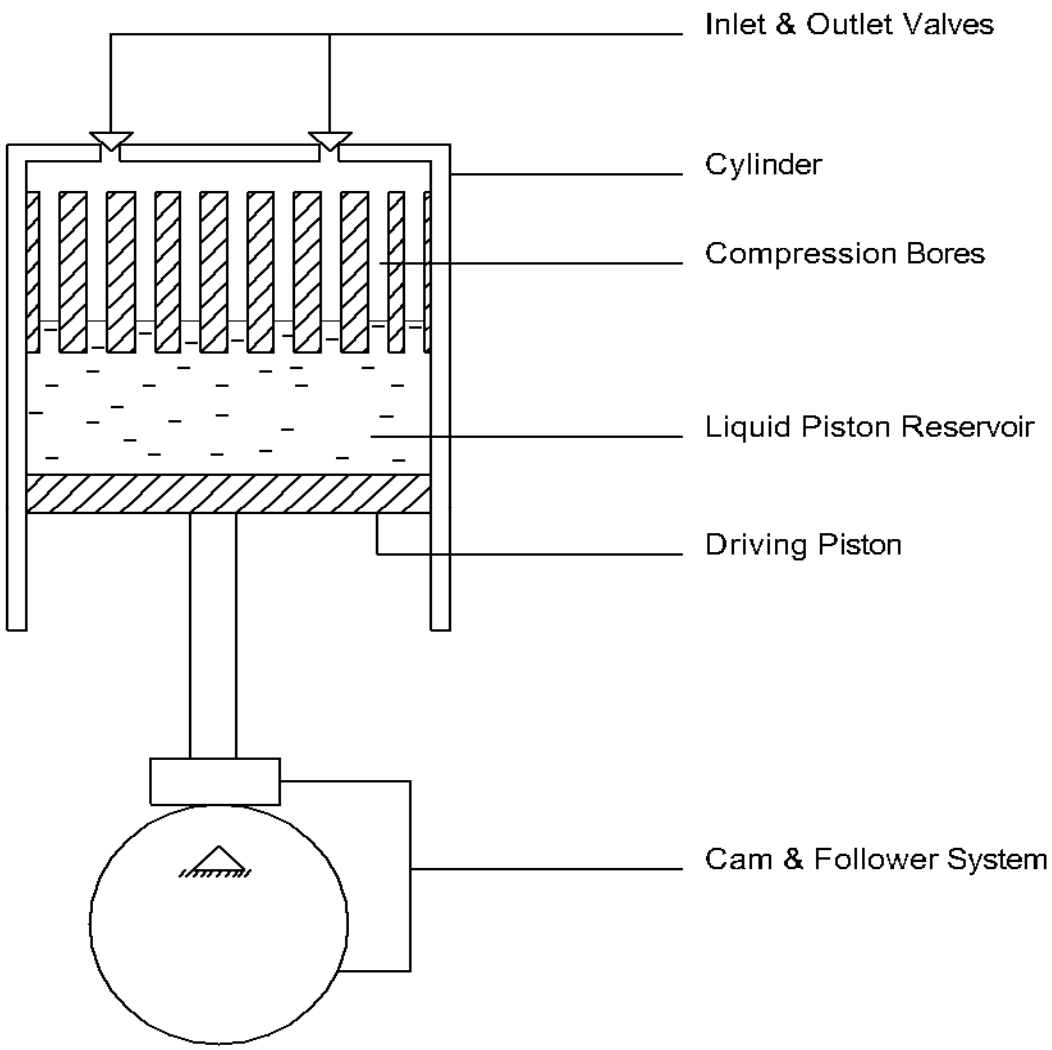

Figure 1. Cross sectional representation of a liquid piston gas compressor driven by a cam-follower system.

The direct advantages associated with the application of this concept in gas compression technologies are an increase in compression efficiencies and a reduction in maintenance and running costs resulting from a decrease in the number of mechanical parts used in the system. Furthermore, this concept also eliminates the need for large external heat exchangers due to the liquid piston's ability to absorb large quantities of heat energy on its own, thus preventing large temperature increases within the system. Additionally, the liquid piston concept allows the gas compression technologies to improve some of the performance characteristics, and design and manufacturing features. It does so by eradicating the sliding frictional losses associated with solid pistons, minimizing gas leakages typically observed in solid seal systems, lowering operation noise and vibrations, and increasing manufacturability by reducing the number of moving mechanical components in the system. Moreover, because a liquid can conveniently

conform into a space with an irregular volume, a liquid piston allows the shape of the working chamber to be modified and to include internal complexities so that heat transfer during compression can be further optimized.

For a preliminary analysis, a single bore from the system was selected and the thermal fluid behavior associated with system fluids contained within the bore during a single compression stroke was studied. This behavior is represented by a numerical model developed in MATLAB, which also allows investigators to study the impact of different physical parameters upon the performance of the system. The goal of the research project is to optimize the system by maximizing heat transfer out of the working gas during its compression so that an isothermal mode of operation can be achieved.

This investigation paper will guide the reader through the system design, literary review conducted for developing a numerical model, and the use of the model for analyzing the effects of physical property changes on the efficiency and performance of the system. The ultimate goal is to fully understand the system operation and quantify the compression efficiencies found within a single-bore of the liquid piston gas compressor.

Literature Review & Background Research

Understanding the physics behind the operation of the liquid piston engine was conducted through research into the fluid dynamics and heat transfer concepts relevant to the system. This section will identify the major properties that dictate the operation of the system and those that affect its overall performance.

Flow Characteristics of System Fluids

During the compression half of a system operation cycle, the liquid piston and the working gas exhibit differing flow patterns. The working gas predominantly shows a unidirectional flow towards the closed end of the system cylinder during its compression. The liquid piston flow on the other hand is a part of a predefined oscillatory motion that occurs back and forth within the small diameter bores (duct) of uniform circular cross sectional area. As a result, to determine thermal fluid parameters of the two system fluids, different approaches need to be adopted in order to account for their respective flow characteristics. One of the primary parameters influenced by such flow characteristics is the flow regime.

Flow Regimes

The flow regime that the system fluids experience within the bores primarily governs all of the other crucial thermal fluid parameters and thus needs to be identified at the initial stage of the analysis. The flow regime can be classified as either laminar or turbulent. A laminar flow regime represents an axis-symmetric ordered flow and provides a simpler and more predictable method for quantifying the thermal fluid parameters. The turbulent flow profile on the other hand is associated with severe complexities which most often cannot be represented by clearly defined equations. Furthermore, even though a turbulent flow provides the prospects of greater heat transfer occurring across the fluid boundaries and lower viscous forces opposing the fluid flow, it also entails a strong possibility for the occurrence of an undesirable mixing between liquid and gas volumes within the system. As a result, a strong effort will be made to maintain the flow regimes of both of the system fluids within the laminar region.

When determining the flow regime of a certain flow characteristic, the concept of a Critical Reynolds Number has a strong significance. This number defines the threshold value above which the flow becomes purely turbulent. Awareness of this number enables us to select appropriate values of the system variables in order to ensure a laminar nature within both of the system fluids. Due to the differing flow patterns shown by the two system fluids, different methods were required for calculating the critical Reynolds number corresponding to each specific fluid. These approaches will be discussed in the ensuing sections once the Reynolds number values of the system fluids have been thoroughly examined.

To identify the flow regimes of the two fluids inside the bores of the system, a preliminary Reynolds number calculation was conducted over the length of an entire operation cycle. This calculation is primarily contingent upon the velocity profile of the fluid flow, the physical properties of the fluid, and

the critical dimension (diameter) of the flow chamber. Therefore it was essential that the kinematic parameters be established, system fluids with suitable physical properties be specified, and appropriate dimensions of the bores in the system be approximated before calculating the Reynolds number values.

Kinematic Parameters of the System

There are two primary kinematic parameters associated with the system. The first involves the linear motion characteristics of the liquid piston and the working gas. The second parameter describes the oscillatory features of the system responsible for consistently providing multiple cycles during system operation

Linear Kinematic Parameters

It was assumed that the kinematic profile imparted by the cam – follower system onto the liquid piston was ideally translated into the working gas as well. As a result, the working gas assumes the same instantaneous velocity magnitudes and directions as that of the follower and the liquid piston during operation. For a preliminary analysis, a simple sinusoidal kinematic profile, corresponding to an eccentric cam – follower system, was selected to drive the oscillations of the liquid piston. The following equations illustrate the mathematical relation between the input cam – follower variables and the resulting kinematic parameters exhibited by the system fluids within a single bore of the system (Norton, 2003).

$$s = \frac{h}{2}\left(1 - \cos \omega t\right) \qquad \textbf{(1)}$$

s = Instantaneous displacement of highest level of liquid column in a bore

h = Bore length of a single bore

ω = Constant angular velocity of eccentric cam

t = Instantaneous time during system operation

$$v = \frac{h}{2}\omega\left(\sin \omega t\right) \qquad \textbf{(2)}$$

v = Instantaneous velocity of liquid column/working gas in a bore

Frequency of Operation

The frequency of operation dictates the angular velocity of the cam follower system. As shown in equations 1 and 2, the kinematic parameters of the system are dependent upon this angular velocity. Thus the frequency can be considered as the fundamental kinematic parameter of the system that not only regulates the oscillatory cycles, but also the linear kinematics observed during specific portions of a system operation cycle.

The frequency also determines the total time available for heat transfer to take place from the gas into the bore walls and from the bore walls into the liquid piston. A higher frequency would decrease this time, which results in lower thermal interactions between the system fluids and the bore walls, causing the system to approach an adiabatic mode of operation. At a low frequency of operation, such exposure time is increased, allowing higher amounts of heat transfer to occur. Low frequencies thus assist the system to approach the desired isothermal mode of operation. However, at low frequencies, the high temperatures of the working gas can also gain sufficient time to evaporate a portion of the liquid piston, and thus yield undesirable conditions during the ensuing system operation cycles.

The four frequencies used for the analysis were 20Hz, 30Hz, 40Hz and 50Hz. These values were based upon balanced conditions in which large exposure time between the system fluids and the surrounding bore wall were maintained without giving way to undesirable evaporations.

These kinematic parameters will be taken into account in all of the ensuing analyses, and will be applied to both of the working gases in the system. There needs to exist a strong compatibility between these kinematic parameters and the type of system fluids selected in order to optimize operational outputs. The following section discusses the system fluids selected for analysis.

System Fluids Properties

As mentioned previously, there are two system fluids utilized in the system: a working gas and an incompressible liquid piston.

Working Gas

The type of gas used as the working gas is very important to the operation of the system. The four main physical properties that influence the working gas's thermal fluid behavior during system operation are its density, thermal conductivity, ideal gas constant, viscosity, and specific heat capacity. According to the ideal gas law, a gas with high density tends to maintain its temperature at a relatively low value during compression. Greater thermal conductivity in the gas increases the heat transfer across its boundaries. A high gas constant, which is directly proportional to the specific heat values of the gas, also increases the gas's potential to discharge heat energy from its bulk volume. Moreover, gases with relatively higher dynamic viscosities are crucial to maintain the flow regimes of the gas within a laminar region. Taking all these factors into consideration, air and helium were used to simulate the working gas in the system analysis, since they seem to possess favorable magnitudes of such properties, and are readily available for use. Their relevant properties are shown in Table 1 below.

Table 1: Gas Properties (Engineering Toolbox)

Working Gas	Density (kg/m^3)	Thermal conductivity ($W\ m^{-1}\ K^{-1}$)	Ideal Gas Constant, R ($J\ kg^{-1}\ K^{-1}$)	Dynamic Viscosity (kg/m s)
Helium @ STP	0.18	0.15	2077	0.00001983
Air @ STP	1.2	0.024	287	0.0000021

Liquid Piston

The main parameters of interest concerning the liquid piston are its fluid density, thermal conductivity and coefficient of dynamic viscosity. Since the liquid is considered incompressible in this system, the density of the liquid column within a bore is only used to determine the mass of the column. As shown in Equation 9 the thermal conductivity enables the calculation of the convective coefficient for heat transfer that occurs across its boundaries, and is crucial to keep track of heat energy extracted from the system. The viscous coefficient is utilized to determine the pressure drops resulting from the viscous resistance of the fluid and to check if the liquid exhibits laminar flow characteristics inside a single bore of the system.

Based on their physical properties, water and MOBIL DTE 25 Hydraulic oil were deemed most suitable for the analysis of this system. The properties of these liquids are shown in Table 2.

Table 2: Liquid Piston Properties (Mobil DTE) (Engineering Toolbox)

Liquid	Density (kg/m^3)	Thermal conductivity ($W\ m^{-1}\ K^{-1}$)	Dynamic Viscosity ($kg\ m^{-1}\ s^{-1}$)
Water	1000	0.58	1.16E-03
DTE 25	876	0.21	2.19E-02

It is crucial that these system fluids flow through channels in which they exhibit optimal flow characteristics to ensure ideal operating conditions for the system. The next section provides an overview of the geometric considerations necessary within the bores of the system.

Geometric Parameters

While performing the analysis, the total mass of working gas compressed in a single cycle of the system operation is kept constant. It is assumed that the liquid column in each bore of the system moves across the length of the bore volume. It begins its motion from the base all the way up to the tip of the bore,

initially compressing the gas and subsequently discharging the compressed gas into the storage chamber once the desirable pressure ratio has been attained. Since the diameter of the bores in the system is the critical dimension, it is treated as the fundamental geometric parameter, where most of the analytical focus is place upon.

During analysis, the diameter of the bore was varied to observe how the output parameters would react to a change in the dimensions of the flow channel. The bore diameters selected for analysis of the system are 0.9 mm, 0.5 mm, 0.4 mm, and 0.2 mm. This selection was made by placing primary emphasis on the flow regime of the system fluids, ensuring that a laminar flow would be observed at all times during the system operation. It was initially intended to keep the volumes in each bore of the system a constant as well. However, during the preliminary analysis it was revealed that even a small modification in the diameter of a single bore caused a drastic change in its axial length. Since, for a large stroke length the fluid flow has to cover a longer distance under a specified time frame, the fluid in the bore attains high velocities that induce undesirable turbulence within the flow. Furthermore, a large stroke length would also increase the overall size of the system, compromising its packaging efficiency. For a short stroke length on the other hand, we end up significantly reducing the area of contact between the system fluids and the surrounding bore wall, which adversely affects the heat transfers occurring in the system. Prior research into the liquid piston gas compression concept indicates that an analytically determined stroke length of 39.3 mm creates a balance among the tradeoffs between a long and a short stroke length (Van de Ven and Li, 2008). For smaller bore diameters, in order to compensate for the loss in the volume inside a single bore, the number of bores in the system is increased to ensure that the total working volume of the system cylinder remains constant.

Having established the fundamental kinematic parameters, fluid properties, and the dimensional features, the following method was utilized to determine the instantaneous Reynolds number values of the two system fluids during operation. This section also discusses how the Reynolds number values obtained were examined to ensure that the flow regimes in each system fluid were kept laminar.

Reynolds Number Calculation and Flow Regime Determination

The instantaneous Reynolds number for a flow through a circular duct with uniform cross sectional area can be obtained from the following equation (Kreith and Bohn, 2000).

$$\mathrm{Re}(t) = \frac{\rho * v(t) * d}{\mu} \qquad \textbf{(3)}$$

$\mathrm{Re}(t)$ = Instantaneous Reynolds Number

ρ = Density of working gas

$v(t)$ = Instantaneous linear velocity imparted by cam – follower system

d = diameter of bore

μ = dynamic viscosity of liquid

This equation is pertinent to both liquids and gases, since it is assumed that the linear velocity imparted by the cam onto the follower is transferred into the liquid piston and the working gas without any significant drop in magnitude.

Working Gas

Reynolds Number Calculation

This Reynolds number equation was applied to the two aforementioned working gas selections within a single bore of the system. All possible extremity combinations of the stipulated kinematic and geometric conditions were taken into consideration in order to obtain a complete picture how the Reynolds number values react to system variability. Figure 2 graphically illustrates the instantaneous values of the Reynolds number exhibited by the two working gases during the compression half of an entire system operation cycle.

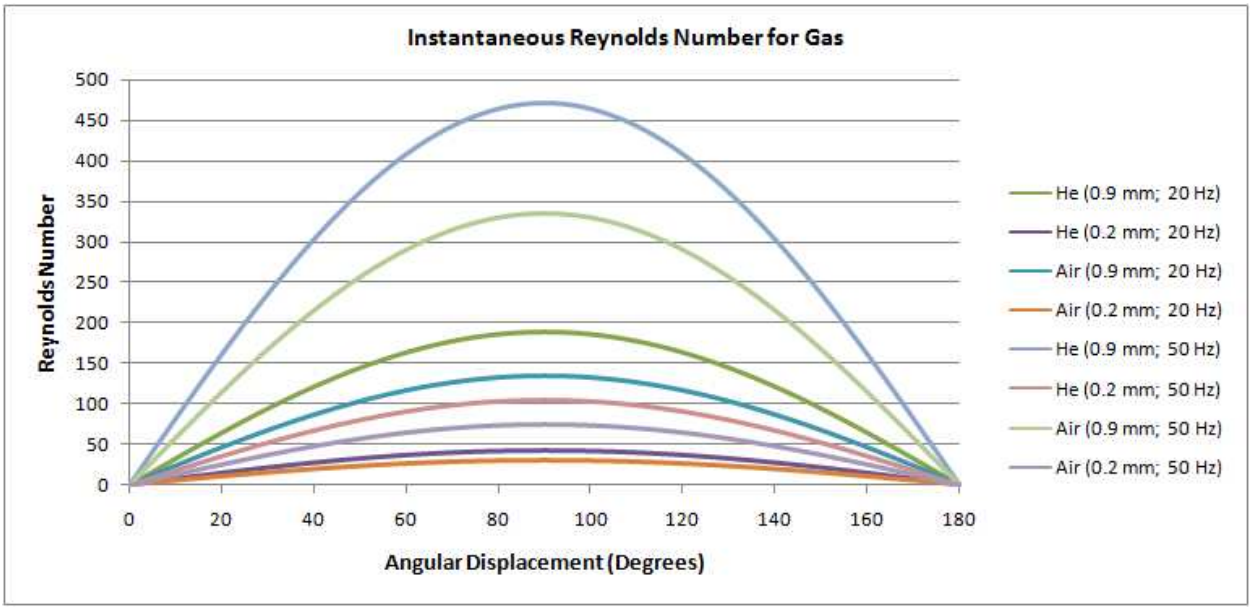

Figure 2: Instantaneous Working gas Reynolds Number Values in a System Cycle

It can be observed that the flow of the working gas is unidirectional and the Reynolds number values are consistently maintained under.

Critical Reynolds Number in Working Gas

The maximum Reynolds number values observed in the working gas in a system cycle need to be compared to the critical Reynolds number values so that the flow regime of the working gases can be

clearly specified. The following table illustrates different ranges of the Reynolds number values where specific flow regimes are observed for a fluid flowing in a constant direction through a duct with uniform cross sectional area (Incropera, DeWitt, Bergman, Lavine, 2006).

Table 3: Flow Regimes Corresponding to Reynolds Number Ranges

Reynolds Number Range	**0 - 2500**	**2500 - 10000**	**over 10000**
Flow Regime	Purely Laminar	Mixed	Purely Turbulent

As indicated in Figure 2, the magnitudes of the Reynolds number values observed in the working gases during system operation are strictly maintained below 400 for all extremity combinations of the kinematic and geometric parameters. As a result, the flow characteristics of the working gases lie significantly below the turbulent threshold and thus exhibit purely laminar behavior.

Liquid Piston

Reynolds Number Calculation

A similar Reynolds number calculation was performed on the liquid piston flowing through a single bore in the system. Both of the liquids considered for analysis were evaluated under all possible extremity combinations of the stipulated kinematic and geometric conditions. The following graph illustrates the instantaneous Reynolds number values for each of such extremity combinations.

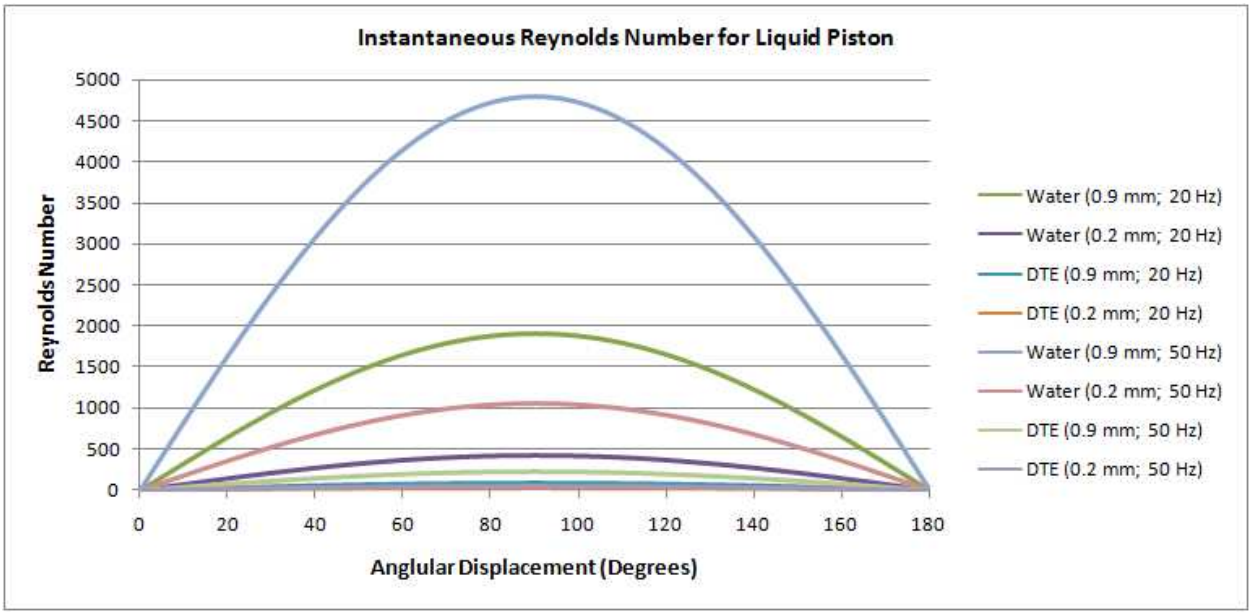

Figure 3: Instantaneous Liquid Piston Reynolds Number Values in a System Cycle

Critical Reynolds Number of Liquid Piston

It can be observed from Figure 3 that the Reynolds number values significantly vary from one parametric combination to another and from one type of fluid to another. However, unlike in the case of a uniform flow, an oscillatory flow corresponding to a specific parametric and liquid combination is associated with a unique critical Reynolds number. This critical Reynolds number for a fluid experiencing oscillatory flow in a cylindrical column can be expressed as follows (West, 1983).

$$\mathrm{Re}_{critical} = 375\left(\frac{D^2\omega\rho}{\mu}\right)^{2/3} \qquad \textbf{(4)}$$

D = bore diameter

ω = angular frequency of the liquid column

ρ = density of piston liquid

μ = coefficient of viscosity of piston liquid

The following table shows the critical Reynolds number pertinent to each parametric and liquid combination. It also shows the maximum instantaneous Reynolds number value observed during a system operation cycle in the liquid piston. It can be seen that this maximum value for all extremity parametric combinations is significantly below the critical value, causing the oscillatory liquid flow to exhibit pure laminar behavior.

Table 4: Comparison between Critical and Maximum liquid Reynolds Number Values in a System Operation Cycle

		Reynolds Number for Extremity Geometric - Kinematic Combinations			
Liquid	**Reynolds Number Type**	**0.9 mm/20 Hz**	**0.2 mm/20 Hz**	**0.9 mm/50 Hz**	**0.2 mm/50 Hz**
Water	**Critical**	7404.96	996.72	13640.05	1835.97
	Maximum	1915.83	425.74	4789.57	1064.35
DTE 25	**Critical**	956.17	128.70	1761.28	237.07
	Maximum	88.89	19.75	222.24	49.39

After establishing appropriate system properties and features that facilitate a favorable laminar regime in the flow characteristics of the system fluids, other thermal fluid parameters relevant to the system operation were evaluated and their significance determined.

Velocity Radius Parameter of the Liquid Column

One of such parameters that define the shape of the radial velocity profile across a liquid column during oscillatory flow through a duct is referred to as the radius parameter of that flow. It is dependent upon the flow column geometry, the viscous properties of the oscillating fluid, and the kinematic parameters of the oscillatory flow. The radius parameter helps us determine the shape of the radial velocity profile observed in the liquid piston during system operation. For a flow through a cylindrical bore, there are two possibilities of the radial velocity profile. The first is a uniform or flat profile, where the fluid velocity is constant across the majority of the bore diameter. The second is a parabolic profile, in which the fluid velocity has a maximum value at the central axis of the bore and progressively decreasing values towards the bore wall. The following figure visually illustrates these radial velocity profiles.

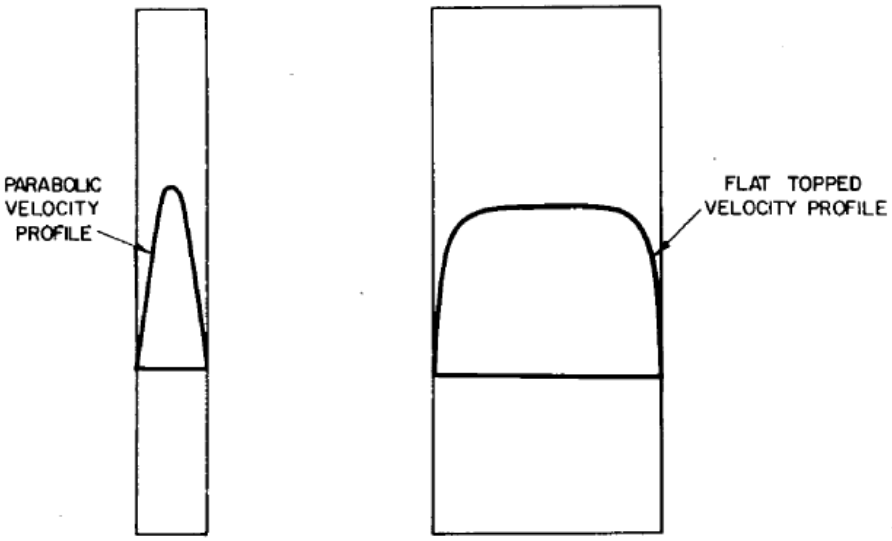

Figure 4: Radial Velocity Profiles Based upon Radius Parameter (West, 1983)

For analysis, the radius parameter associated with a fluid flow can be mathematically expressed as follows (West, 1983).

$$R^* = D\sqrt{\frac{\omega\rho}{\mu}} \qquad \textbf{(5)}$$

$R^* \geq 1$ (flat velocity profile) $\qquad$ $R^* << 1$ (parabolic velocity profile)

As indicated above if the radius parameter is greater than or close to unity, the radial velocity profile across the liquid column is fairly uniform and can be approximated as a flat profile. If it is significantly below unity, then the radial velocity profile attains a parabolic shape during fluid oscillation (West, 1983). The following table shows the radius parameter values associated with various oscillatory liquid flows comprising of different extremity kinematic and geometric combinations, and occurring within the individual bores of the system.

Table 5: Radius Parameters for Extremity Geometric and Kinematic Combinations

	Radius Parameters for Different Geometric - Kinematic Combinations			
Liquid	**0.9 mm/20 Hz**	**0.2 mm/20 Hz**	**0.9 mm/50 Hz**	**0.2 mm/50 Hz**
Water	9.37	2.08	14.81	3.29
DTE	2.02	0.45	3.19	0.71

It can be seen that the majority of the radius parameter values in Table 5 are either greater than one or sufficiently close to one. As a result, while performing numerical analysis for understanding the internal workings of the liquid piston system, it can be assumed that the instantaneous radial velocity profile of a liquid column within a bore of the system is uniform. Such uniformity in the radial velocity profile has important implications especially on the viscous properties of the liquid piston flowing through the bores of the system. The next section will describe this significance in detail.

Viscosity

The use of the liquid-piston concept replaces the frictional sliding losses found in conventional solid piston systems with viscous losses resulting from molecular interactions between the liquid volume and the surrounding bore walls. Such resistances that oppose the motion of the fluid flow can be represented as follows (Fox, McDonald, Pritchard, 2006).

$$F_{viscous} = \tau \cdot A \qquad \textbf{(6)}$$

τ = fluid shear stress

A = surface area of contact between fluid and cylinder wall

The instantaneous sheer stress for a Newtonian fluid is evaluated using equation 7, which relates sheer stress to the dynamic viscosity and the instantaneous velocity gradient orthogonal to the direction of flow.

$$\tau = \mu \cdot \frac{du}{dy} \quad \textbf{(7)}$$

μ = fluid dynamic viscosity

$\frac{du}{dy}$ = flow velocity gradient across bore diameter

As shown in the previous section, it is reasonable to assume a uniform velocity profile across a single bore in the system with a sharp decline at a close proximity to the bore wall. This causes the fluid velocity gradient to approach zero through the majority of the liquid piston volume and attain a significant magnitude right next to the walls. Therefore, the resulting viscous forces experienced by the system fluids at the bore walls are generated along the interface that separates the bore wall from the liquid volume. For analytical purposes, the viscous loss associated such flows, where the radial velocity is predominantly uniform, can be determined from the following equation (Fox, McDonald, Pritchard, 2006). This equation replaces the differential change in velocity in the viscosity equations with the average velocity per unit radial length value observed across the bore.

$$F_{viscous} = A \cdot \mu \cdot \frac{v(t)}{(d/2)} \quad \textbf{(8)}$$

A = surface area of contact between wall and fluid

μ = fluid dynamic viscosity

v(t) = velocity of liquid column imparted by cam

d = diameter of bore

This force is utilized to calculate the negative work done by it during compression. The negative sign of this work indicates an opposing nature of the viscous force and also suggests that energy is being consumed by the force from the system.

Cavitation

Alongside viscous losses, the formation of gas pockets – cavitation – is another phenomenon encountered when studying liquid and gas interaction.

Cavitation is usually observed at regions where the local pressure of a flowing liquid falls below its vapor pressure, causing gaseous pockets to appear within its volume. If these pockets are close to a mechanical component and they happen to collapse or rupture, they can potentially release high

magnitude destructive energies, in the form of shock waves, causing severe damage to the component (Brennen, 1995).

In the case of the liquid piston technology, the formation of gas bubbles inside the liquid column can be caused by spontaneous mixing between small portions of the liquid and gas volumes. In spite of its different origin, this phenomenon produces similar destructive physical effects and is thus also referred to as cavitation due to the lack of a better terminology. On the whole, formation and the ensuing collapse of gas bubbles – cavitation- in liquid compression devices have been known to decrease their performance and efficiency, and increase operation vibration and noise (Brennen, 1995).

Cavitation can normally be avoided by ensuring that the pressure within the liquid column never goes below the pressure of the gas. Therefore, any head loss or frictional loss that could lower the pressure of the liquid column must be minimized. Frictional (fluid viscosity) losses can be minimized by increasing the diameter of the bore or decreasing the length of travel. An alternate method is reducing the temperature of the liquid to prohibit its mixing with the gas (Brennen, 1995). The last and most difficult method is to maintain a permanent physical boundary between the liquid and the gas, which could be achieved by using a highly elastic solid layer such as a thin film or a highly viscous fluid as the separation membrane.

Having taken into account all the crucial fluid dynamics phenomena that could potentially be observed during system operation, the thermodynamic and heat transfer processes will now be discussed to provide a more coherent picture of the system.

Heat Transfer during Gas Compression

One of the primary operational parameters of the liquid piston system that this project intends to accurately represent is the heat transfer occurring out of the system during gas compression, so that appropriate measures can be taken to optimize its magnitude. The heat transfer in the system occurs in the following forms.

Convection

Inside the bores of the system, there exists an interface between the system fluid volume and the surrounding bore wall enclosing those fluids. As the working gas in a single bore gets compressed during system operation, its temperature progressively increases, giving rise to a temperature difference between the gas and the surrounding bore wall. This temperature difference induces a flow of heat energy from the working gases into the surrounding wall. Similarly, during this compression stage, the liquid piston gradually moves upwards along the system bore, increasing its area of contact with the surrounding bore wall. Because the liquid is maintained at a fairly low temperature, it tends to absorb significant amounts of heat energy from the surrounding bore wall. Both of these heat transfers are equivalent to a forced convection occurring inside a circular duct, and are associated with specific values

of coefficient of convection. This value can be mathematically obtained from the following expression (Kreith and Bohn, 2000).

$$h = \frac{Nu * k}{D} \quad \textbf{(9)}$$

h = convection coefficient for the given gas – surface interface

Nu = Nusselt number associated with the fluid flow

k = conduction coefficient of the gas

D = diameter of the liquid column

This equation makes the assumption that the flow through the duct is uniform and laminar, and is associated with minimal energy losses associated with viscosity. We know from the previous sections, that the laminar flow and minimal losses assumption is highly viable for the liquid piston system. The uniform flow characteristic applies accurately to the working gas, but is not representative of the oscillatory nature of the liquid piston. However, if we make the assumption that the convective heat transfer occurs only when the liquid column velocity is non zero and that the oscillatory motion doesn't involve any dwell periods, the analysis focuses at only the unidirectional flow segments of the liquid piston oscillations.

As a result, the underlying assumptions apply to both of the system fluids, making this equation applicable to both fluids in determining their convective coefficients of heat transfer. According to the concept of forced convection inside ducts, flows that are purely laminar tend to have Nusselt number values that are extremely close to an average value. This average Nusselt number is equivalent to 4.36 (Kreith and Bohn, 2000). Therefore, this value is used for calculating the convection coefficient of the given fluid – surrounding wall interface.

The direction of convective heat transfer is orthogonal to the bore axis. As a result, the convective heat transfers are classified as the radial heat transfer of the system. This heat transfer can be numerically quantified through the following expression (Incropera, DeWitt, Bergman, and Lavine, 2006).

$$Q_{rad} = h.A_s.(T_{from} - T_{to}) \quad \textbf{(10)}$$

Q_{rad} = Quantity of radial heat transfer

h = convective coefficient

A_s = Surface area of heat transfer interface

T_{from} = Temperature of heat energy source

T_{to} = Temperature of heat energy destination

Conduction

The second form of heat transfer that occurs within the system is restricted entirely to the material surrounding the system fluids. It is true that conduction is also observed in the system fluids, but its relative magnitude is so low that it can be safely assumed negligible to simplify analysis. As mentioned previously, during the compression stage the liquid volumes in the bores consistently absorb heat energy from the surrounding bore walls they make contact with. Since the liquid piston moves from the bottom of the bore towards its top, the lower regions of the surrounding bore walls remain in contact with the liquid volume for a longer period of time. As a result, the nether regions of the surrounding bore walls have lower temperatures compared to the upper regions. Such temperature difference along the length of the surrounding bore wall creates an axial temperature gradient across its entire body. During system operation, this axial temperature gradient causes heat energy to flow from regions at higher temperature to regions at lower temperature. Since this heat transfer occurs through a consistently uniform material within the bore walls, it is classified as pure conduction and occurs in a direction opposite to the compression of the working gas. Because of such axial flow characteristics, it is referred to as an axial heat transfer and can be expressed by the following equation (Incropera, DeWitt, Bergman, and Lavine, 2006).

$$Q_{axial} = \frac{k.A}{L}.(T_{from} - T_{to}) \qquad \textbf{(11)}$$

Q_{axial} = Quantity of axial heat transfer

k = Conduction coefficient of the surrounding material

A = Cross sectional area of surrounding material

L = Distance of heat transfer

T_{from} = Temperature of heat energy source

T_{to} = Temperature of heat energy destination

During system operation, both radial and axial heat transfers occur simultaneously and thus significantly influence the thermal characteristics of the system. One of the goals of the project is to check how various parameters and variables pertinent to the system can be varied in order to facilitate higher quantities of heat transfer out of the working gas in order to help increase the efficiency of gas compression. Different approaches towards such analysis will be explained thoroughly in the following section.

Heat Transfer Analysis

While performing heat transfer analysis, different components of the system under consideration were classified as either a total bulk volume or a collection of finitely discretized volumes. In either case the classification was selected based upon the precision requirements of the heat transfer analysis and the level of convenience desired.

Bulk Volume Method

In the bulk volume method, the system is divided into distinct components in which each component is treated as a single unit that has uniform physical, thermal, and chemical properties across its volume. During operation of the system, if any changes are induced into the properties of a certain component, the change occurs at the same rate and extent throughout its volume. While performing heat transfer analysis, if a bulk volume of a component gains or loses a certain amount of heat energy, the temperature of the entire volume will change to accommodate the heat transfer.

This method of heat transfer analysis allows the formulation of convenient heat transfer models where an approximate thermal interaction behavior between various components of a system can be observed. If the precision requirements of the system are less stringent and provide room for various assumptions to be made, this method of analysis is highly desirable. Furthermore, from a preliminary design and modeling perspective, this method can be invaluable in gaining insight into the system being worked upon.

Finite Difference Method

In the finite difference method, the total volume of a system component is divided into a finite number of sub volumes. The size of each one of such sub volumes is made small enough to facilitate uniform physical, chemical, and thermal properties within them at all times. As a result, each sub volume or discretized element can be represented by a single point node, positioned at its geometric center. Under such conditions, the total volume of a system component is represented by a nodal network rather than its geometry.

During operation of the system, the adjacent nodes within a nodal network interact with one another as separate units and exhibit changes in their properties due to such interaction. Consequently, during analysis the finite difference method facilitates the numerical representation of non – uniform property distribution and changes across the total volume of a system component. The results of this method can be optimized by discretizing the total volume into a large number of small differential volumes. This causes the nodes in the nodal network to reside very close to one another and provides a stronger representation of the property distribution across the system component volume (Incropera, DeWitt, Bergman, and Lavine, 2006).

During system analysis, both of these heat transfer analysis methods were utilized in specific contexts, based upon their effectiveness in providing accurate and conveniently obtainable results.

Thermodynamic Analysis

This analysis is utilized to quantify the instantaneous values for the gas temperature during compression. It basically comprises of two crucial thermodynamic concepts that dictate the thermal parameters of the working gas during compression. This section describes these two concepts.

Energy Balance Equation

This equation basically states that the total change in energy within a compressed fluid is equivalent to difference between the heat transfer associated with the fluid and the mechanical work imparted into it induce the compression. During the system's operation, the working gas is associated with a unique energy balance equation during each incremental time step. This energy balance equation can be generically established through the following expression (Cengel and Boles, 2001).

$$\Delta E = Q - W \qquad \textbf{(12)}$$

ΔE = Total change in energy within working gas during each incremental compression

Q = Heat transfer out of the working gas during each incremental compression

W = Work done by liquid piston to induce incremental compression

Ideal Gas Law

The other thermodynamic concept that is utilized in the analysis is the ideal gas law. This concept provides a basis for comparing the instantaneous pressure, volume and temperature of the working gas. It is essential that such relations between the three thermodynamic parameters be known, since the efficiency calculations of the system are contingent upon them. The following equation represents the ideal gas law.

$$\frac{P * V}{T} = k \qquad \textbf{(13)}$$

k = constant

P = Instantaneous pressure of working gas

V = Instantaneous volume of working gas

T = Instantaneous temperature of working gas

Methodology

With all the fundamental concepts established, a working model that represents the internal thermal fluid characteristics of the system can now be developed. This section describes various approaches taken towards the formulation of this model.

Single Bore Approach

Before venturing into the development of the working model for the system, it is crucial to first understand the fundamental unit of analysis in the system. As mentioned previously, the total liquid piston volume is distributed among a large number of small diameter bores. Since the majority of the thermal fluid interactions of the system components occur within these bores, they need to be treated as the fundamental units of analysis. In this section, a single bore is fully described and analyzed so that it creates a basis for the ensuing working model. The following material provides the rationale behind the use of such bores in the system.

Heat Transfer Enhancement

The main mode of heat transfer occurring within the liquid piston system is convection. Since the Nusselt number in the system is considered to be a constant, the coefficient of convection becomes a function of the bore diameter. As a result the only means of increasing the heat transfer out of the working gas is by increasing the area of contact between the working gas and the system cylinder and by maintaining the temperature of the system cylinder at a lower value. When the primary working chamber within the system cylinder is divided into a large number of bores - visualized in Figure 5. Each bore adds a certain amount to this surface area of contact, creating conditions more conductive towards heat transfer from the working gas into the system cylinder. Furthermore, with this concept the area of contact between the liquid piston and the system cylinder also proportionally increases, allowing the system cylinder to discharge greater quantities of heat energy it absorbed from the working gas into the liquid piston, and thus helping maintain the temperature of the system cylinder at a relatively low value.

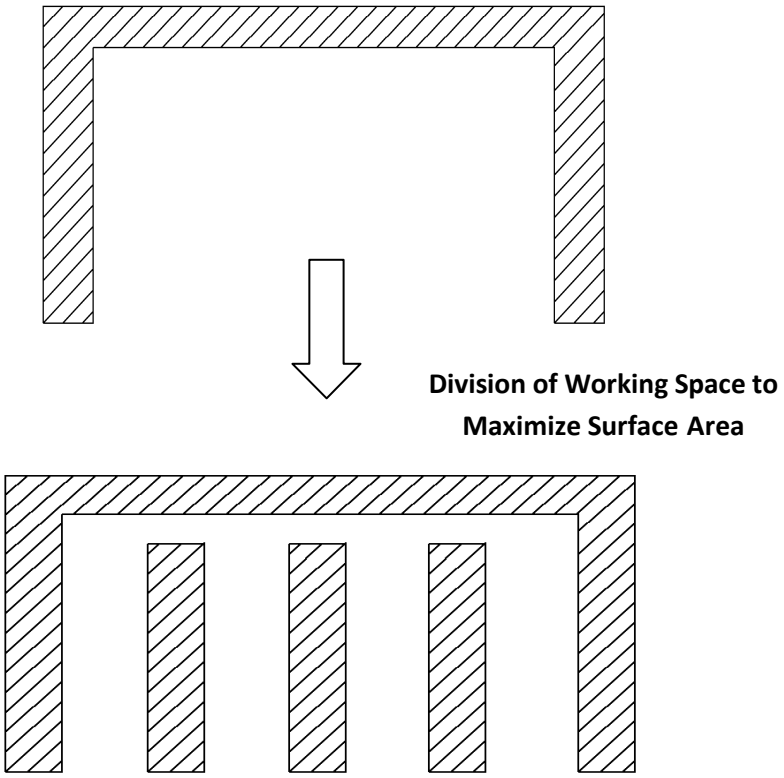

Figure 5: Division of a cylinder into a multi-bore system.

Flow Characteristics Improvement

The other crucial implication of dividing the working chamber into a large number of small diameter bores is the possibility of strictly maintaining the flow regime of both system fluids within the laminar region. As described in the previous sections, the small diameter bores prohibit turbulent behavior within the fluid flows, by tightly constricting them within a narrow region. Furthermore, the low contact area allowed between the liquid and working gas volumes by the narrow diameters in each bore, contributes towards the prevention of the mixing of the two fluids and the evaporation of the liquid volume. These features play a significant role in prohibiting the occurrence of undesirable gas entrapment within the liquid volume and cavitation of the liquid piston.

Having justified the need for the bores of the system, we can now proceed towards analyzing the thermal fluid processes taking place inside the bores during system operation. But before performing the analyses, it is crucial that the physical attributes of the single bore model be thoroughly understood. The following sections describe such properties and the methods used in determining them.

Single Bore Dimensional Modeling

For the purpose of a first-order analysis, only a single bore is taken into account in the working model. Figure 6 illustrates visually represents such a single bore.

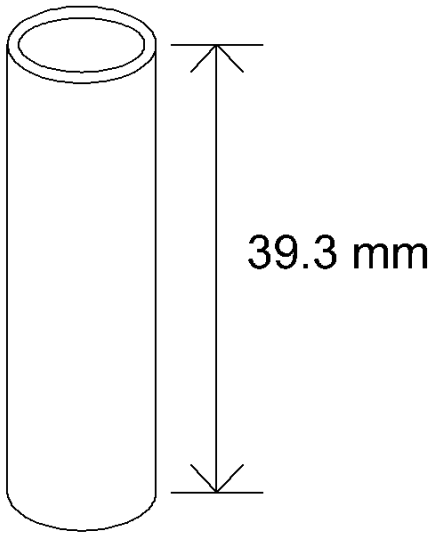

Figure 6: Single cylindrical bore.

For analytical purposes, such a single bore is assumed to resemble a hollow cylindrical structure. Its length and diameter values are as specified in the previous section titled – Geometric Parameters. For specifying the thickness of the single bore, a dimensional analogy was made to a hypodermic needle. The scaling factor was obtained by taking the ration of the diameter of the hypodermic needle to its wall thickness. Upon applying this scaling factor to the average bore diameter being used in the analysis, it was concluded that an appropriate wall thickness of the single bore model is 0.488 mm.

Single Bore Components

The single bore basically comprises of three components.

a) **Surrounding Bore Wall:** This component consists of a solid material that lies on the outermost region of the bore and serves as a rigid boundary that encases the contents of the bore. For a preliminary analysis, steel with a density 7850 kg/m^3 was selected as the metal that constituted the surrounding bore wall. This wall was assumed to be perfectly insulated from the surrounding environmental conditions, preventing thermal interactions between the single bore and the environment. This assumption was crucial in order to limit the focus on the analysis within the single bore, and to avoid unnecessary complexities induced by including variables associated with the surrounding environment

b) **Liquid Piston:** As mentioned in the previous sections, water and hydraulic fluid Mobil DTE 25 were used as separate liquid piston choices.

c) **Working Gases:** During the compression half of a system cycle, the two separate choices of working gases (Air and Helium) were assumed to exhibit ideal gas characteristics. This assumption helped simplify the calculation of various thermodynamic parameters entailed in the analysis.

Figure 7 shows the cross sectional view of a single bore along with its constituent components.

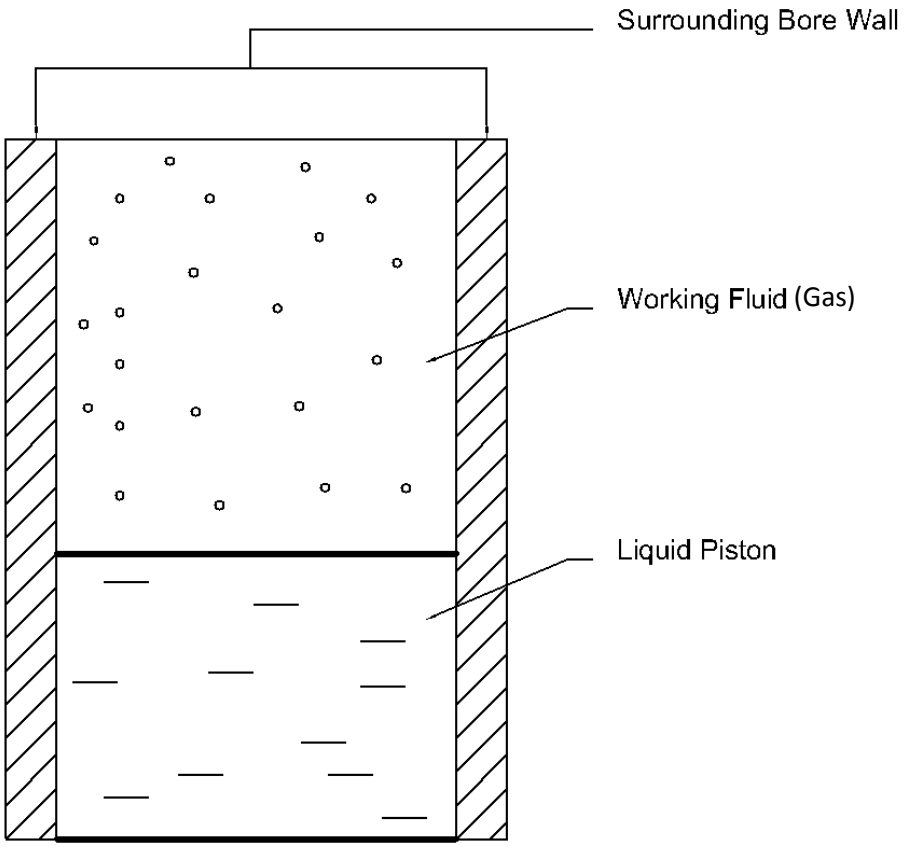

Figure 7: Sectioned view of a single bore.

At this point, sufficient information has been obtained about the single bore model. The following section describes the internal workings in a single bore of the system during system operation in a generic manner. The detailed analyses and methods will be discussed in the other sections devoted purely to the system analysis.

Internal Workings of a Single Bore

Initially, the temperature of the surrounding bore wall and the working gas are maintained at 298 Kelvin. The temperature of the liquid column – regulated though external cooling - is kept constant at

288 Kelvin to encourage greater radial heat transfer from the bore walls. As the liquid column is forced upwards by the cam-follower system, the volume of the working gas gets reduced due to compression. The result is an increase in the bulk gas temperature. With increasing working gas temperatures, a temperature differential is engendered at the gas – wall interface, causing radial heat transfer between the two to occur.

As this compression progresses, the upper regions of the single bore tend to develop higher temperatures than its lower regions, since the upper regions are predominantly in contact with the hot working gas and the lower regions with the cold liquid piston. As a result, a temperature differential is established across the length of the surrounding bore wall. This initiates a second mode for heat transfer to occur within the single bore. Such heat transfer is conductive in nature, occurring downwards along the axial length of the surrounding bore wall. The axial heat transfer allows the upper regions of the surrounding wall to "cool" itself, and thus helps maintain consistent axial heat transfer into those regions from the working gas.

The third mode of heat transfer occurs when the liquid column in a single bore comes in contact with the surrounding bore walls during compression. Since the liquid column is maintained at a lower temperature, radial heat transfer from the wall into the liquid is initiated, decreases the wall temperatures at the lower bore regions. Figure 8 illustrates this trend of semi-cyclic heat transfer occurring within the single bore in the compression half of the system cylinder.

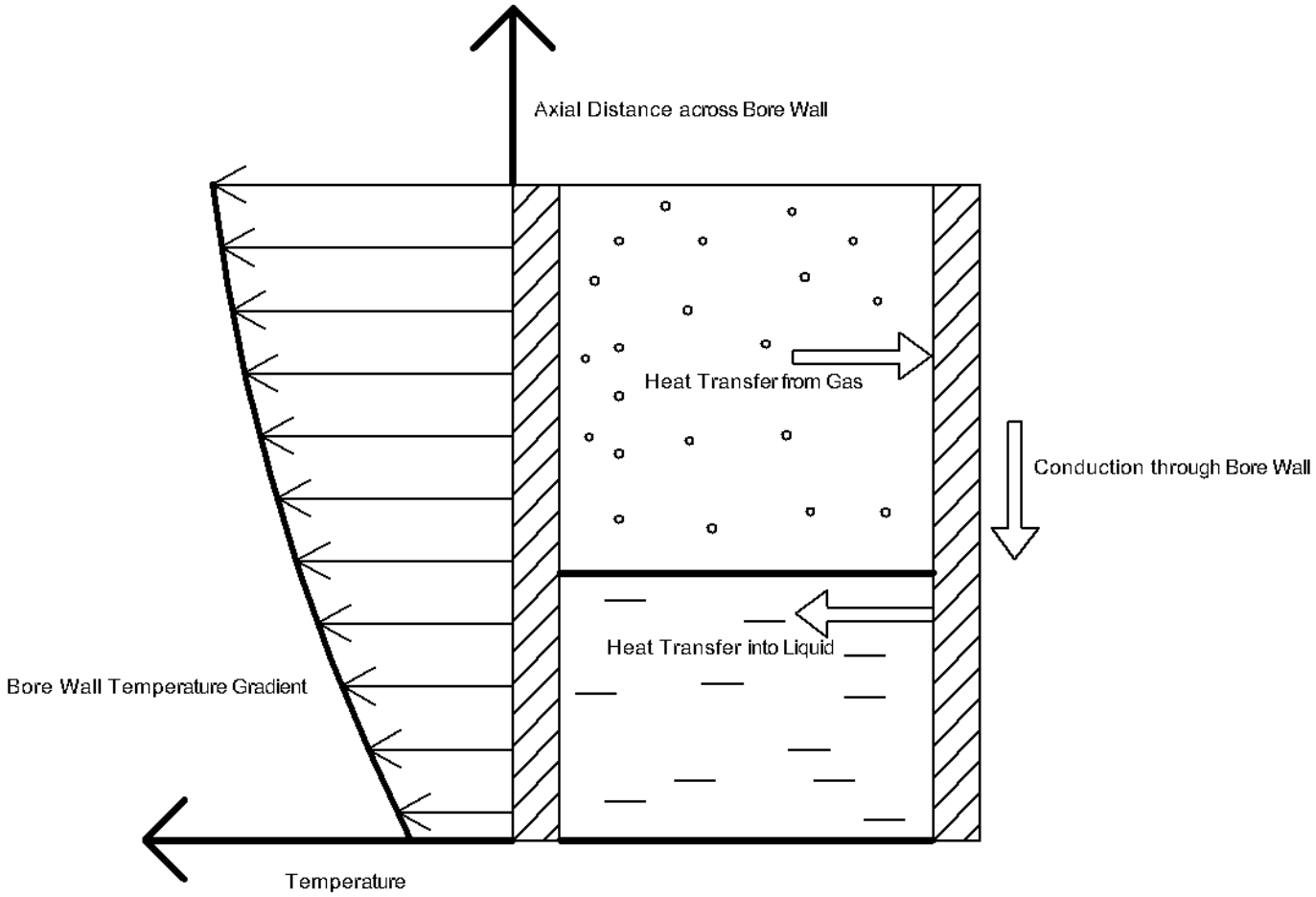

Figure 8: Heat transfer process and wall temperature gradient.

It can be concluded that the axial heat transfer across the bore length and the radial heat transfer from the surrounding bore wall into the liquid column work together to maintain a high temperature differential between working gas and the surrounding bore wall. This causes an increase in the heat energy dissipated from the working gas during its compression. Consequently, the power required to perform the compression is reduced since a low temperature gas provides less resistance to the compressive forces exerted by the liquid piston. Such a phenomenon has a direct positive effect on the efficiency of the system. This efficiency can be made ideal if the radial heat transfer from the working gas can keep the system under an isothermal condition.

The following sections describe the models that utilize the Single Bore Approach for performing system operation analyses.

Preliminary Model

In the preliminary model established to analyze the internal thermal fluid behavior of the liquid piston system, an attempt was made to associate the instantaneous thermal-fluid parameters of the system fluid with the external kinematic parameters that facilitate the operation of the liquid piston. In this approach, the liquid column within a single bore was treated as a bulk volume that experiences a resultant inertial force due to the application of external forces acting on it during operation. These external forces can be classified as follows.

1. **Cam System Forces**: This is the force exerted by the driving cam – follower system onto the bulk liquid volume within a single bore. The magnitude of this force varies with the displacement of the liquid volume across the bore, since it encounters various types of opposing forces.

2. **Viscous Forces:** As a liquid column rises along its respective bore, the molecular interactions occurring at the interface between its bulk volume and the surround bore material result in viscous forces that oppose its upward motion.

3. **Gas Forces:** During the compressive stage of the system operation, the compression of the working gas causes its internal pressure to significantly increase. Such progressively increasing gas pressure impinges onto the liquid piston volume at the gas – liquid interface, and acts in a direction that opposes the liquid piston's inward motion across the bore.

4. **Bulk Volume Weight:** This force is a result of gravity acting upon the vertically positioned bulk volume of the liquid piston within a single bore. Since the bulk volume during compression progressively increases with displacement, this force is also a variable force

5. **Inertial Forces:** When the effects of all the aforementioned forces are combined at every single instance during the compressive stage, the algebraic sum results in a total force that is responsible for the upward motion of the liquid piston. This can expressed as the product of the instantaneous mass and acceleration of the bulk volume within a single bore.

The instantaneous inertial force acting on the bulk liquid volume in a single bore is illustrated below by the free body diagram in Figure 6 and equation 12.

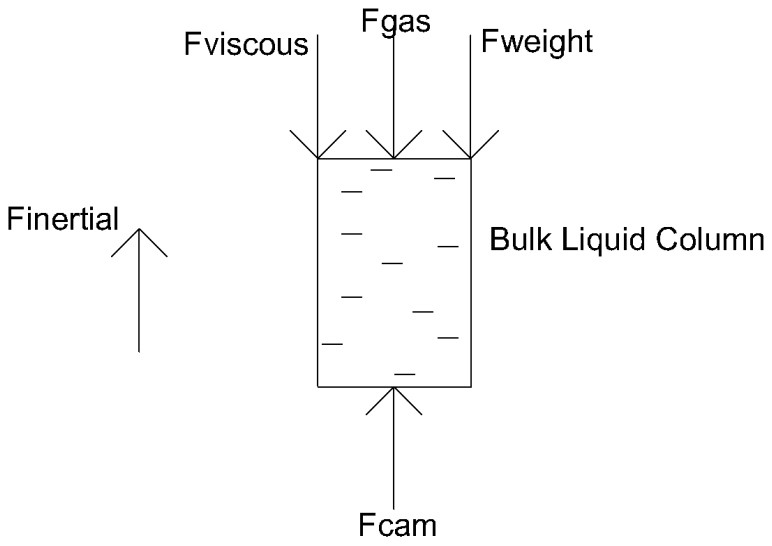

Figure 9: Free body diagram of bulk liquid column.

$$F_{cam} - F_{viscous} - F_{gas} - F_{weight} = m(t) * a(t) \qquad \textbf{(14)}$$

All values of the parameters in the equation pertain to a specific instance within a single bore during the operation of the system.

In this model all of the primary external forces, except the cam forces, could be mathematically represented through either thermodynamic or kinematic concepts associated with the operation of the system. The cam exerts a unidirectional force on the follower to maintain the stipulated kinematic profile. If the cam is robust enough, it will endure any form of opposing forces to prevent digression from that profile. As a result, the magnitudes of the cam forces exhibit significant vacillations, making its representation highly complex. Therefore, this analysis was abandoned and a simpler one sought after. The following section describes the methodology used in an alternative approach

Numerical Analysis

This approach placed primary emphasis on the thermodynamic behavior of the working gas and didn't require us to keep track of external forces acting on the system. It was found that if the energy balance equation pertinent to gas compression in the system is manipulated appropriately, the temperature of the compressed fluid becomes the only unknown variable in the equation. This equation can be thus solved to obtain instantaneous temperature values of the working gas during compression. In the numerical analysis, the total compression of the working gas during a single operating cycle of the

system is divided into a finite number of incremental compressions. The energy balance equation when applied to each one of such incremental compressions allows us to keep track of the working gas temperature at various instances during compression. These known instantaneous values of the working gas temperature form the basis for the computation of other thermal fluid parameters relevant to the system.

The fundamental concepts entailed in the numerical analysis of the internal thermal fluid behavior of the liquid piston system are the finite difference method and the bulk volume method. Since a single bore of the system is being used as the primary unit of system analysis, these concepts were applied to the appropriate components of a single bore. In order to accommodate the numerical analysis, the components of a single bore were classified as follows:

Working Gas Bulk Volume: Since the working fluid is a gas, it has the ability to rapidly change its properties across its volume and can thus be treated as a single bulk volume with uniform thermal – fluid properties.

Liquid Piston: This volume is treated as a collection of discretized differential elements, each interacting independently with a specific surrounding wall differential volume that it makes physical contact with.

Surrounding Wall Metal Volume: As indicated by its name, this volume encompasses the metal region surrounding the working gas and the liquid column within a single bore. It is discretized into a number of differential volumes in order to facilitate numerical analysis. This volume is further sub-classified into two regions based on the fluid it makes contact with.

1. **Gas Contact Volume:** This region of the surrounding metal volume makes direct physical contact with the working gas. Since the volume of the working gas progressively decreases during the compressive stage of the system operation, the volume of this region also exhibits proportional decrease in magnitude.

2. **Liquid Contact Volume:** This region of the surrounding metal volume maintains contact with the liquid column in a single bore. During the compression stage of an operation cycle of the system, this region gains volumetric magnitude as the liquid column rises from the base position to its maximum displacement.

Having specified the primary components of the system and designated appropriate geometric classification to each one of them, the ensuing steps in the numerical analysis entailed the establishment of various nodal network associated with the discretized components of the system. The following section describes the process involved in the nodal network set up.

Discretization of System Components

Figure 10 shows the cross sectional vertical view of a single bore during the compressive stage of its operation. There are basically three types of nodal networks set up in this single bore.

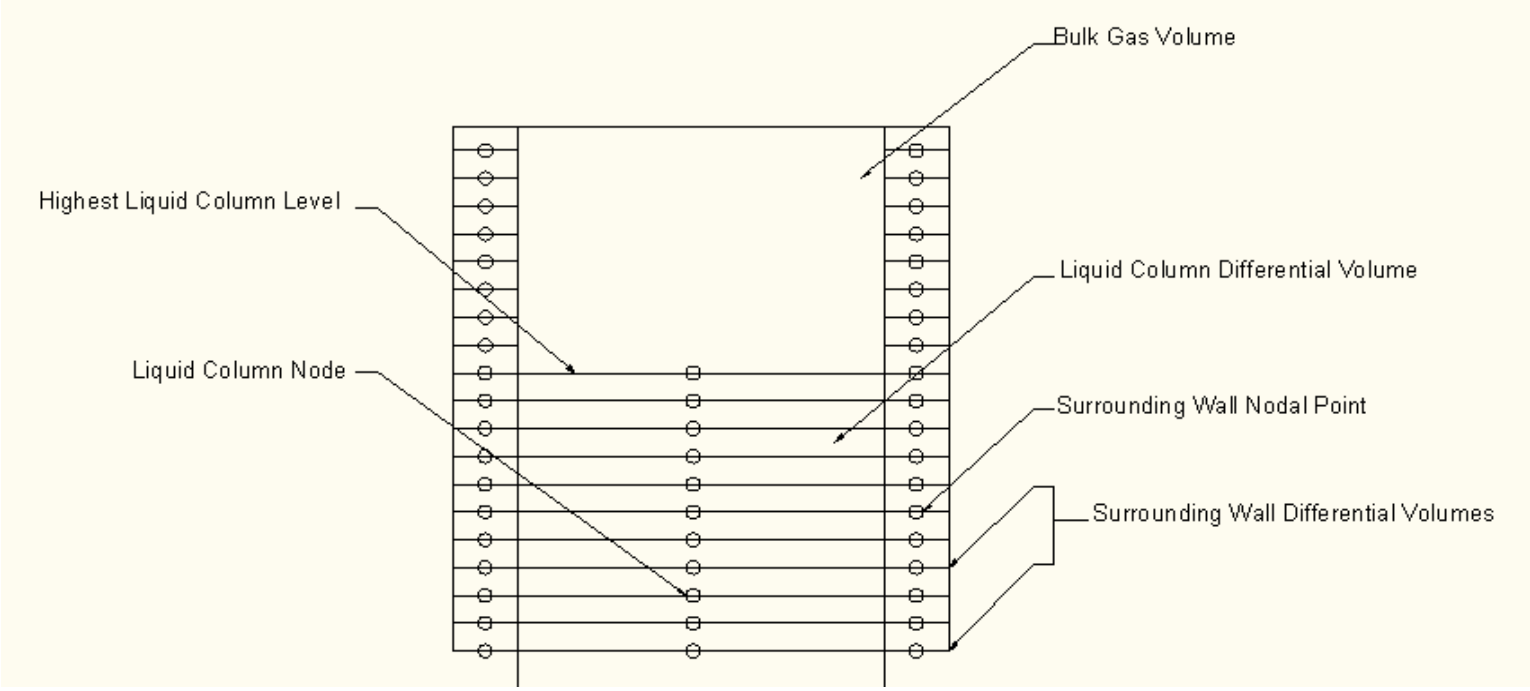

Figure 10: Nodal network of a single bore during compression stage.

Liquid Column Nodal Network: As indicated in the figure, the liquid column moves upwards during the compression stage, traversing the spaces designated for individual differential volumes and supplanting spaces previously occupied by the working gas. Such designated spaces are equally spaced across the entire length of the bore and thus allows each incremental compression associated with a single differential volume to be equal to one another. The nodal point of each differential volume in the liquid column is assigned at its upper limit along its central vertical axis. The lowest level of the liquid is also assigned a particular node (referred to as the 0 node) and associated with initial conditions prevalent during the compression stage.

Surrounding Wall Nodal Network: This nodal network is created across the entire volume of the cylindrical bore surrounding the working gas and the liquid piston. It basically comprises of annular shaped solid differential volumes with a uniform thickness similar to that of the liquid column differential volumes. The nodal points are placed at the upper limits of each of such differential volumes along a straight vertical line that lies within the volume of the surrounding wall and passes across its length. This network is utilized for calculating the convectional heat transfer occurring between the two fluids and the surrounding wall, and the conductional heat transfer taking place across the length of the surrounding wall.

In the numerical analysis, the system component volumes were not the only parameters discretized. The predetermined total time period taken by the system for completing a single compression stroke across a bore was also discretized into a finite number of equally spaced time periods. During each one of such

infinitesimal time periods, the liquid column moves across a certain number of nodes within the system and induces heat transfer to occur through change in thermal properties of the system components.

Numerical Heat Transfer Analysis

As mentioned previously, all heat transfers occurring within the system can be classified as either radial or axial based upon the direction of heat energy flow. The following sections describe each directional heat transfer in detail and derive mathematical expressions for quantifying heat transfer magnitudes occurring during system operation.

Axial Heat Transfer across Bore Length

When calculating axial heat transfer values, it is highly desirable that the pattern of heat energy transfer throughout the surrounding wall be observed and strictly controlled. Therefore, this heat transfer analysis is conducted through the finite difference method and is applied across the nodal network prevalent within the surrounding wall. During analysis, it is assumed that axial heat transfer occurs in incremental values between adjacent nodes. There are two specific conditions that dictate the form of axial heat transfer occurring within a single bore. These conditions are based upon the relative position of the nodes pertinent to each incremental axial heat transfer occurring within the system. The axial heat transfer occurs in and out of each surrounding wall node at specific time-steps. Each specific positional node and time step is designated by the integer variable 'j' and 'i' respectively. In all mathematical representations, the subscript on a certain variable represents a specific time step, while the superscript represents the node under consideration. The following figure illustrates the numerical representation of nodes relative to one another in terms of geometrical position.

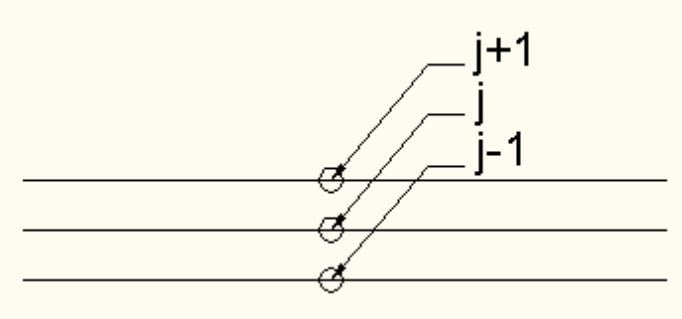

Figure 11: Nodal Numbering

The axial heat transfer occurring within the bore walls entail two specific conditions pertaining to the relative position of the nodes being analyzed within their nodal networks. The following section describes these conditions in detail and stipulates appropriate heat transfer equations pertinent to them.

Condition 1: When heat energy is transferred between adjacent nodes residing within the surrounding wall of a single bore, it is classified as pure conduction and can be quantified by the following mathematical expressions.

$$Q^{j}_{axial,out,i} = \frac{\Delta t \cdot k \cdot A_{ring} \cdot (T^{j-1}_{metal,i} - T^{j}_{metal,i})}{L} \quad \textbf{(15)}$$

$$Q^{j}_{axial,in,i} = \frac{\Delta t \cdot k \cdot A_{ring} \cdot (T^{j+1}_{metal,i} - T^{j}_{metal,i})}{L} \quad \textbf{(16)}$$

$Q^{j}_{axial,out,i}$ = Heat energy dissipated by a node to a lower adjacent node

$Q^{j}_{axial,in,i}$ = Heat energy absorbed by a node from a higher adjacent node

Δt = Incremental time step

A_{ring} = Annular cross sectional area of surrounding wall in a single bore

k = Coefficient of conduction of the surrounding wall material

L = Distance between adjacent surrounding wall nodes

$T^{j-1}_{metal,i}$ = Instantaneous temperature of a lower adjacent node

$T^{j+1}_{metal,i}$ = Instantaneous temperature of a higher adjacent node

$T^{j}_{metal,i}$ = Instantaneous temperature of a node under consideration

As it can be seen from equations 13 and 14, heat transfer occurs into and out of each node within the surrounding wall. It is assumed that the top most node is perfectly insulated from the top, causing it to only dissipate heat energy to its lower regions and not interact thermodynamically with the environment above it.

Condition 2: For the lowest node positioned at the interface between the surrounding wall of a single bore and the primary liquid volume below the single bore, out-flowing axial heat transfer occurs in a convective form and can be determined from the following expression.

$$Q^{1}_{axial,out,i} = \Delta t \cdot h_{liquid} \cdot A_{ring} \cdot (T_{liquid} - T^{1}_{metal,i}) \quad \textbf{(17)}$$

h_{liquid} = Convective coefficient of heat transfer for the liquid

T_{liquid} = Constant temperature of the liquid

These two heat-transfer quantities are classified as Qin and Qout. These heat transfer values cause a temperature change to occurs at each node. This change is dictated by the following equation:

$$Q_{in} + Q_{out} = M_{metal} \cdot C_{metal} \cdot (T^{j}_{metal,i} - T^{j}_{metal,i-1}) \quad \textbf{(18)}$$

$$T^{j}_{metal,i} = \frac{(Q_{in} + Q_{out})}{M_{metal} \cdot C_{metal}} + T^{j}_{metal,i-1} \quad \textbf{(19)}$$

M_{metal} = Constant mass of each surrounding wall differential volume

C_{metal} = Specific heat capacity of surrounding wall material

$T^{j}_{metal,i}$ = Temperature at a specific surrounding wall node at a specific time step

$T^{j}_{metal,i-1}$ = Temperature at a specific surrounding wall node at a previous time step

Radial Heat Transfer across Bore Cross Sectional Planes

This heat transfer occurs between the surrounding wall and the fluids contained within the bore. The heat energy flow is restricted along planes that are parallel to the bore cross section and directed from a higher temperature zone to a lower temperature zone. Such radial heat transfer occurring as a result of the interaction between the surrounding wall and the fluids can be classified under two different conditions, depending upon whether the interaction is across a wall-gas interface or a wall-liquid interface.

Condition 1: Radial Heat Transfer across Wall – Gas Interface

This condition describes the instantaneous heat transfer that occurs from the compressed gas into the surrounding wall that makes contact with the working gas. Because a temperature gradient is induced by the axial heat transfer across the length of the surrounding wall, each differential volume of the gas contact region has a different temperature differential with the working gas and thus absorbs a different amount of heat energy during a specific incremental compression. The following expression shows how the instantaneous radial heat transfers occurring after each incremental compression can be mathematically determined.

$$Q_{r,gas \rightarrow wall} = \sum_{j=l}^{n} \left[h_g \cdot A_s \cdot \Delta t \cdot (T^{j}_{metal,i-1} - T_{gas,i}) \right] \quad \textbf{(20)}$$

$Q_{r,gas \rightarrow wall}$ = Total radial heat transfer from working gas to surrounding wall

h_g = Convective coefficient of heat transfer for working gas

$T^{j}_{metal,i-1}$ = Temperature of a surrounding wall differential volume in previous time step

A_s = Surface area of a differential working gas – surrounding wall interface

$T_{gas,i}$ = Instantaneous temperature of working gas

l = Lowest node of surrounding wall in contact with working gas

n = Highest node number of surrounding wall

The summation indicates that the radial heat transfer occurring at each differential volume of the surrounding wall making contact with the working gas is being added up to obtain a total value. This value can be expanded and represented as follows.

$$Q_{r,gas\rightarrow wall} = h_g \cdot A_s \cdot \Delta t \cdot \sum_{j=l}^{n} T^{j}_{metal,i-1} - h_g \cdot A_s \cdot \Delta t \cdot (n-l) \cdot T_{gas,i} \qquad \textbf{(21)}$$

During each incremental compression corresponding to a specific time step "i", the working gas volume is undergoing thermodynamic changes that can be illustrated by the energy balance equation within its volume.

Having established the expressions to represent the heat energy removed from the working gas during its compression, an effort to keep track of its thermodynamic parameters during each time step was made. This is made possible through the use of the energy balance equation, which is discussed in the following section

Energy Balance Equation

As shown in Equation 13 the energy balance equation is divided into three components. These three components pertinent to the liquid piston system are treated individually in the following sections.

a) Total Change in Working Gas Energy

The following expression provides a mathematical representation of the total change in the energy of the working gas when subjecting it to a certain thermodynamic process (Cengel and Boles, 2001).

Change in working gas energy = Change in internal energy + Change in gas kinetic energy

$$\Delta E = C_v.M(T_{gas,i} - T_{gas,i-1}) + \frac{1}{2}M\left(v_f^2 - v_i^2\right) \quad \textbf{(22)}$$

C_v = Specific heat capacity of working gas

$T_{gas,i}$ = Working gas temperature at a specific time step

$T_{gas,i-1}$ = Working gas temperature at a previous time step

M = Mass of working gas

v_i = Working gas velocity at the beginning of a specific time step

v_f = Working gas velocity at the end of a specific time step

b) Heat Transfer from Working Gas

As indicated in the previous section, the total heat transfer occurring during each incremental compression is equivalent to the radial heat transfer from the working gas to the surrounding wall making contact with the gas as stated in equation 18.

$$Q_{gas} = Q_{r,gas \to wall}$$

c) Work Done on Working Gas

Work done on a gas by a compressive input force is equivalent to the product of its average pressure during the compression and its change in volume resulting from the compression.

$$W = P\Delta V$$

$$W = \rho.R.T_{gas,i}.\Delta V$$

$$W = \frac{M}{A.(h - s_f)}.R.T_{gas,i}.A.(s_i - s_f) \quad \textbf{(23)}$$

W = Work done on working gas during an incremental compression

P = Instantaneous pressure inside the working gas

ΔV = Change in working gas volume in an incremental compression

ρ = Instantaneous density of working gas

R = Molar gas constant of working gas

A = Cross sectional area of bore

s_i = Initial position of liquid column at a specific time step

s_f = Final position of liquid column at a specific time step

When the three components of the energy balance equation are combined together, it can be observed that the only unknown variable is the instantaneous working gas temperature. Therefore, this variable can be isolated and expressed as a function of the other known or predictable parameters during the system's operation. The generic instantaneous working gas temperature equation gets reduced to the following form.

$$T_{gas,i} = \frac{(M.C_v.T_{gas,i-1}) + (h_g.A_s.\Delta t.\sum_{j=l}^{n} T^j_{metal,i-1}) - \frac{1}{2}.M.(v_i^{\,2} - v_f^{\,2})}{(M.C_v) + \frac{M.R.(s_f - s_i)}{h - s_i} + \left[h_g.A_{s,i}.\Delta t.(n-l)\right]} \qquad \textbf{(24)}$$

The radial heat transfer induces an increase in temperature in the surrounding wall volume that is in contact with the working gas. The instantaneous temperature of this surrounding wall volume is given by E25. This equation is derived from the heat addition/removal in solids formula.

$$Q^j_{gas,i} = M_{metal}.C_{metal}.(T^j_{metal,i-1} - T^j_{metal,i}) = h_g \cdot A_s \cdot \Delta t \cdot (T^j_{metal,i-1} - T_{gas,i})$$

$$T^{bulk}_{metal,i} = \frac{Q_{gas}}{M_{metal,i}.C_{metal}} + T^{bulk}_{metal,i-1} \qquad \textbf{(25)}$$

$Q^j_{gas,i}$ = Radial heat transfer into a specific surrounding wall differential volume

Condition 2: Radial Heat Transfer across Wall – Liquid Interface

The second form of radial heat transfer that occurs within a single bore system is also convective in nature, except that it takes place between the liquid column and the surrounding wall. In the analysis pertinent to this heat transfer, it is imperative that the surrounding wall in contact with the liquid column be discretized into a number of differential volumes that are represented by point nodes. This is because the points surrounding wall in the bore, during the compressive stroke, are exposed to the gas or the liquid within the bore for different intervals of time. As a result, certain regions of the surrounding wall receive longer exposure to the lower temperature liquid and are thus compelled to dissipate higher amounts of heat energy during system operation.

As a result of this phenomenon, the cross boundary heat transfer between the liquid column and the surrounding wall in contact with the liquid is analyzed for each individual node. The heat transfer expression in equation 25 shows the quantification of an infinitesimal heat exchange between geometrically corresponding liquid and surrounding wall nodes.

$$Q_{liquid} = Q_{r,liquid \rightarrow wall} = h_{liquid}.A_{wall}.\Delta t.(T_{liquid} - T^{j}_{metal,i}) \quad \textbf{(26)}$$

Q_{liquid} = Radial heat transfer from a liquid node into a corresponding surrounding wall node

h_{liquid} = Convective coefficient of heat transfer of the liquid

A_{wall} = Differential surface area of liquid – surrounding wall interface

T_{liquid} = Constant liquid temperature

$T^{j}_{metal,i}$ = Surrounding wall temperature of a specific nodal position during a specific time period

This radial heat transfer reduces the temperature of each differential surrounding wall volume making contact with the liquid column. The following equation shows how these nodal temperatures change in values during each time step.

$$T^{j}_{metal,i} = \frac{Q_{liquid}}{M^{nodal}_{metal}.C_{metal}} + T^{j}_{metal,i-1} \quad \textbf{(27)}$$

$T^{j}_{metal,i-1}$ = Surrounding wall differential volume temperature at previous time step

M^{nodal}_{metal} = Mass of a single differential surrounding wall volume

Efficiency Evaluation

The final efficiency of the system is determined based on the energy retained by a single batch of working gas compressed in a single bore after it has been cooled down to ambient temperature. Because the working gas after being compressed is cooled at constant pressure, it undergoes isobaric expansion in the storage chamber. During expansion it releases a certain amount of energy, which can be quantified by using the ideal gas law.

$$\frac{V_{compressed}}{T_{compressed}} = \frac{V_{cooled}}{T_{ambient}}$$

$$E_{loss} = P.\Delta V = P_{compressed}.(V_{cooled} - V_{compressed}) \quad \textbf{(28)}$$

$V_{compressed}$ = Volume of the working gas immediately after undergoing compression

V_{cooled} = Final volume of the working gas after being cooled

$T_{compressed}$ = Working gas temperature immediately after undergoing compression

T_{cooled} = Working gas temperature after being cooled

This loss in energy is thus utilized to determine the final efficiency of the system.

$$Efficiency = \frac{W_{input} - E_{loss}}{W_{input}} \times 100 \quad \textbf{(29)}$$

W_{input} = Total input work

It will be shown in the ensuing sections that about 99 – 100% of the input energy are utilized towards compressing the working gas. As a result, energy losses other than the temperature drop losses can be neglected from the analysis.

Results

The Matlab model was used to identify how varying diameters and operation frequencies affected the system performance during compression. Water and Mobil DTE 25 hydraulic fluid were used to simulate the liquid piston while the gas was represented by air and helium. Combinations of the two gases with the two liquids were run with each varying parameter as displayed in the test matrix in Table 6. The following results were obtained from the tests.

Table 6: Matrix of all test combinations.

	Water	DTE 25
Air	Bore Diameter	Bore Diameter
	Operating Frequency	Operating Frequency
Helium	Bore Diameter	Bore Diameter
	Operating Frequency	Operating Frequency

The bore diameters used for the system were 0.2, 0.4, 0.5 and 0.9 mm. The system was operated at 20, 30, 40 and 50 Hz.

The results are analyzed using graphs that have been produced by running the Matlab simulation and are arranged accordingly:

- Impact of varying bore diameters on gas temperatures
- Impact of varying frequencies on gas temperatures
- Impact of varying bore diameters on radial heat transfer
- Impact of varying frequencies on radial heat transfer
- Viscous Pressure Drops

Furthermore, the absolute efficiencies of comparison and total heat transfer quantities have been calculated and categorized in a table for immediate comparison.

Impact of varying bore diameters on gas temperature

Figure 12 represents the complete gas temperature plot for a single compression stroke, involving a 180 degree rotation of the cam. There are two significant characteristics to the temperature plot. An inflection point at 128 degrees represents the transition from the compression to the constant pressure expulsion of the gas. Prior to the point of inflection, a rise in temperature is associated with the compression of the gas. After the inflection, as the gas is forced out of the cylinder, the temperature gradually approaches its initial value. However, at the second point of interest occurring in this case at 178 degrees, the graph approaches an almost asymptotic rise to 2100 Kelvin. This is associated with a numerical error in the simulation, which even after considerable revision has been difficult to avoid. Due to the very small mass of the working gas at the final stages of compression, the algebraic equations begin to lose coherence with the accurate physical phenomenon. In the remaining report, the gas temperature plots have been modified to eliminate the effects of the numerical errors towards the end to provide more clarity.

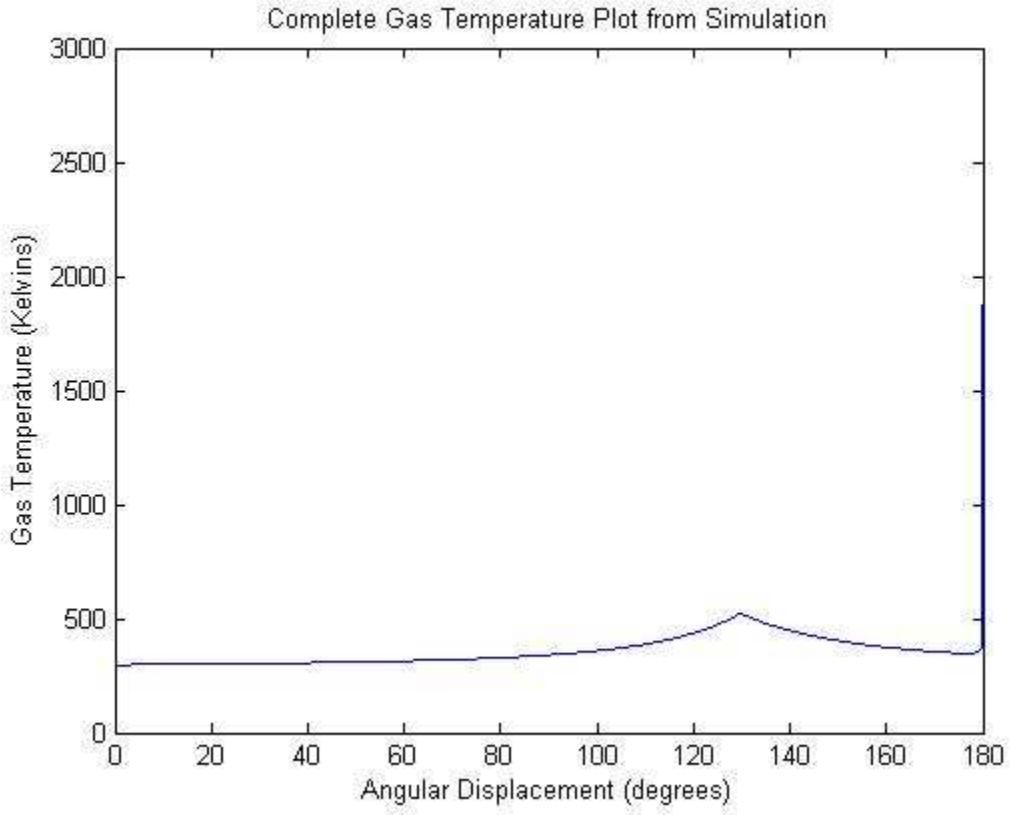

Figure 12: Complete Gas Temperature Plot

Figure 13 through Figure 16 display the gas temperature profiles due to variations in the diameters when the system was run at 20 Hz operating frequency. The arrow indicates the direction of decreasing

diameter in each graph. As mentioned previously, to clarify the graphs and omit the numerical errors towards the final stages, the temperature plots have been restricted to view until 170 degrees of cam rotation.

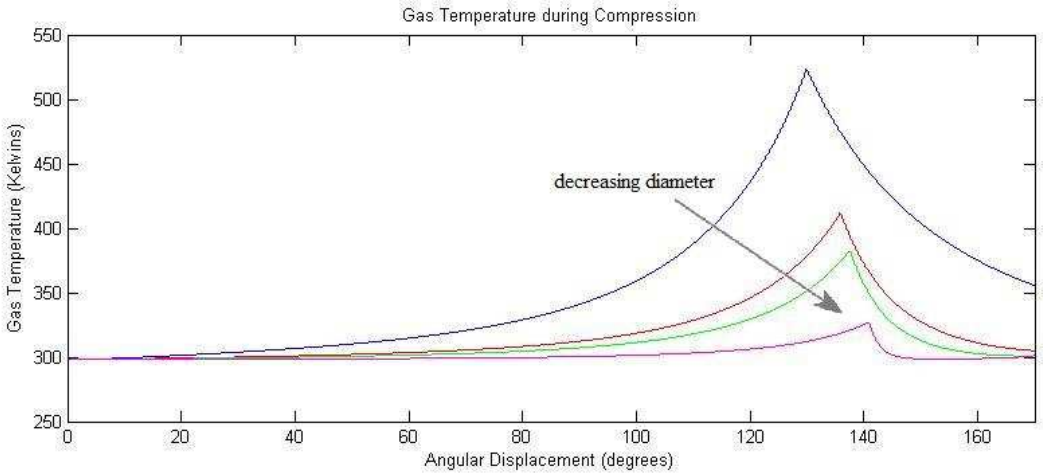

Figure 13: Gas temperatures at varying diameters in an air and water system.

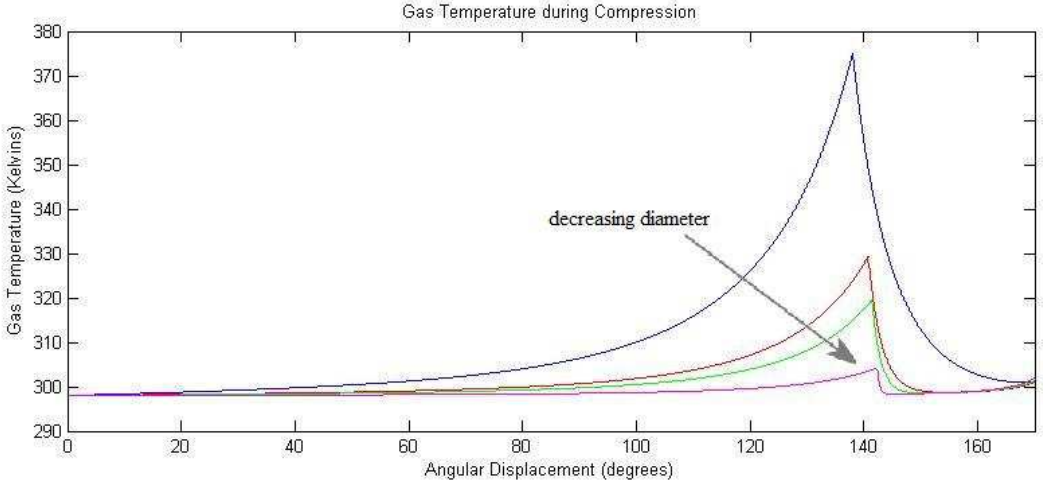

Figure 14: Gas temperatures at varying diameters in a helium and water system.

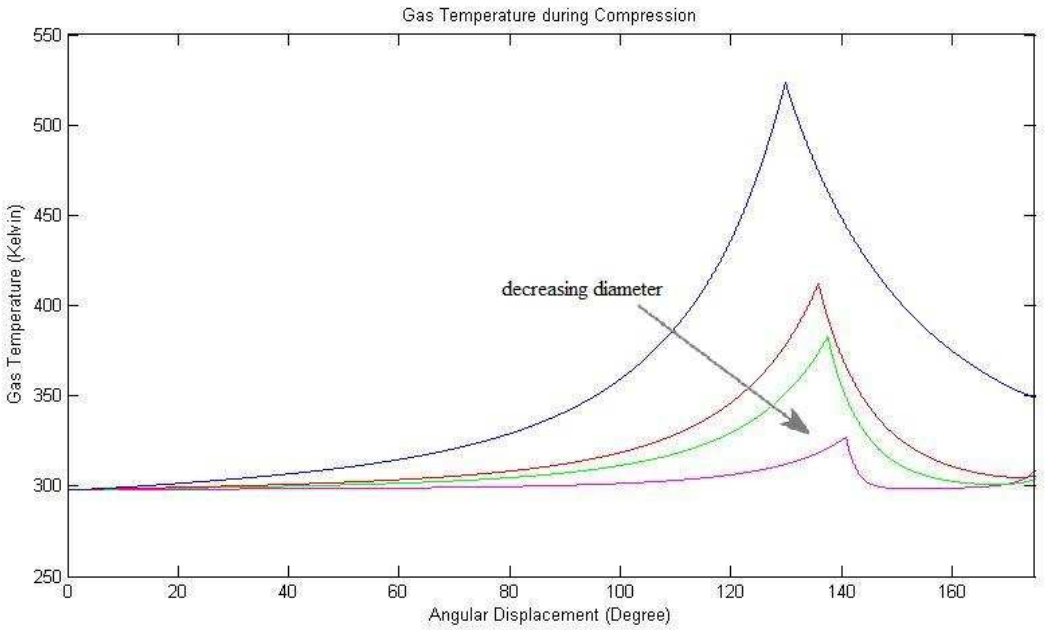

Figure 15: Gas temperatures at varying diameters in an air and DTE 25 system.

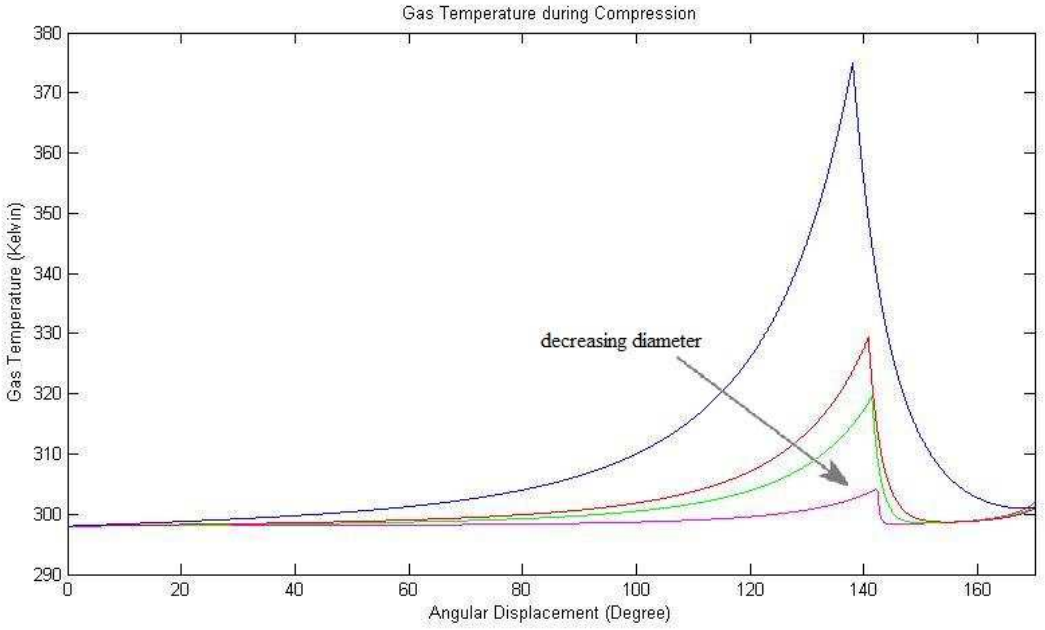

Figure 16: Gas temperatures at varying diameters in a helium and DTE 25 system.

The figures show that as the bore diameters increase, the gas temperatures also increase. Once the pressure ratio of 9.8 is reached, the gas begins to cool and approach a constant temperature. The rate of cooling is greater as the diameters decrease. It is also important to note that the temperature of the gas at smaller diameters approaches the initial temperature of the system more readily than in the larger

diameter systems. The rate of cooling is also drastically greater for a system using Helium as the gas. The gas is cooled most effectively during expulsion when DTE25 is used in combination with the helium as the liquid piston and working gas respectively.

Impact of varying operation frequencies on gas temperature

Figures 17 through 20 show the impact of varying frequencies on the gas temperature while the bore diameter was held constant at 0.9 mm.

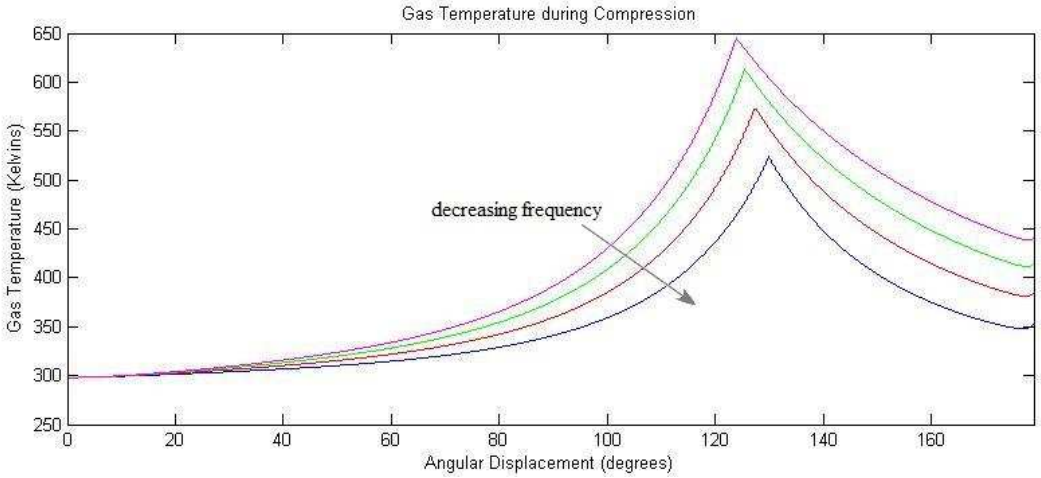

Figure 17: Gas temperatures at varying frequencies in an air and water system.

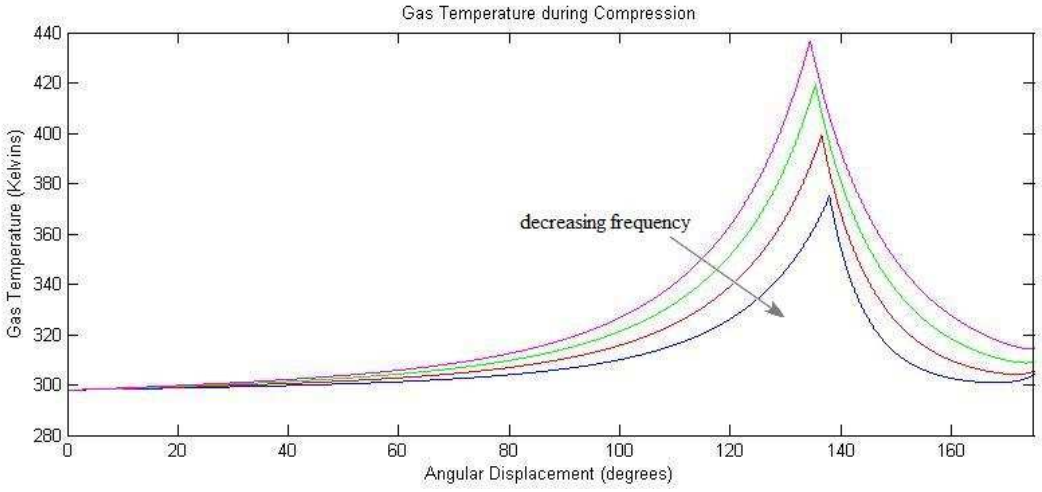

Figure 18: Gas temperatures at varying frequencies in a helium and water system.

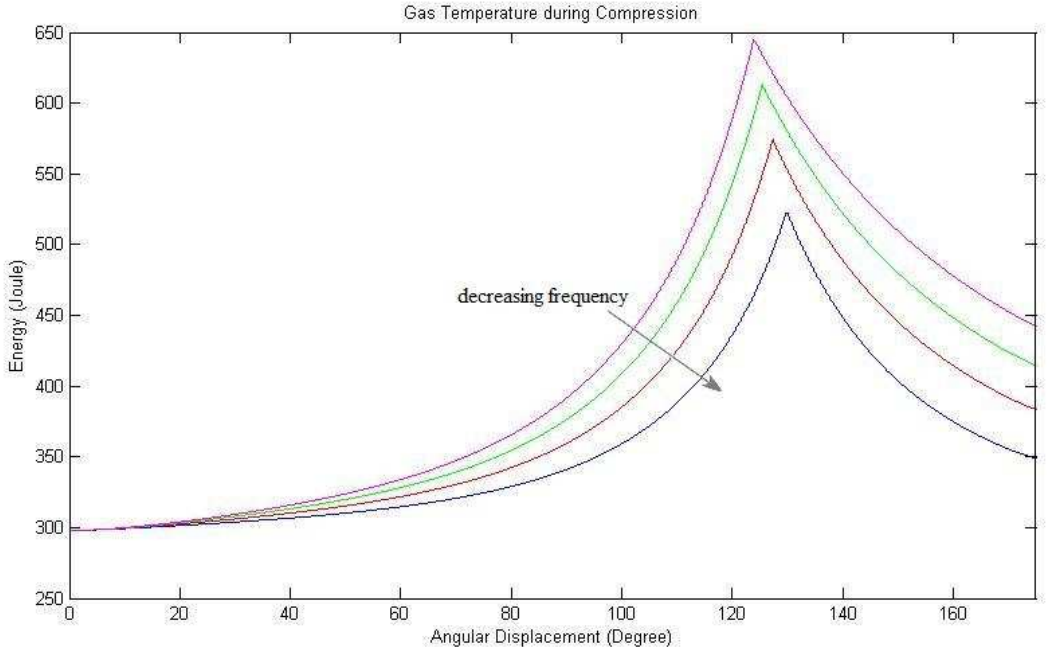

Figure 19: Gas temperatures at varying frequencies in an air and DTE 25 system.

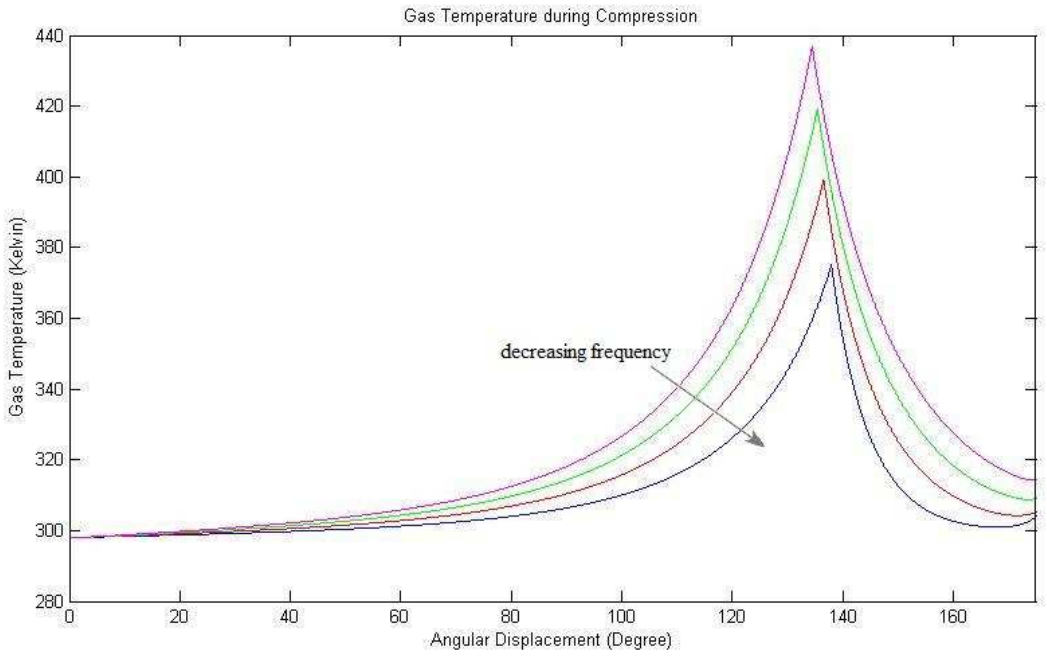

Figure 20: Gas temperatures at varying frequencies in a helium and DTE 25 system.

As expected, a higher frequency of operation forces higher gas temperatures to occur during compression. Once again, the system using helium as the working gas achieves lower gas temperatures.

Impact of varying bore diameters on radial heat transferred

The plots for radial heat transfers occurring to and from the surrounding walls at the differing bore diameters have been organized according to the gas and liquid piston combinations below. All heat transfer quantities were equated with a constant frequency of 20 Hz and the plots show the heat transfer quantities for one complete compression cycle.

Figures 21, 23, 25 and 27 display the quantity of heat transfer occurring from the working gas to the surrounding bore. As the gas becomes hotter during compression, the heat transfer quantities also increase exponentially. The radial heat transfer from the gas is increased along with increased bore diameters – a consequence of the higher gas temperatures attained. The radial heat transfer quantities from the gas are higher for the system using helium by a magnitude of ten. It is interesting to note that the radial heat transfer profile occurring from the gas to the surrounding wall is similar to the temperature profile for the gases viewed above.

On the other hand, Figures 22, 24, 26 and 28 display the quantity of radial heat transfer into the liquid column from the surrounding bore wall. Once again, an increasing bore diameter produces greater quantities of heat transfer. A comparison between the four figures distinguishes the performance of water as a liquid column from DTE 25 as a liquid column. It is clear that water contains the ability to absorb greater quantities of heat energy in comparison to DTE 25.

Air-Water System

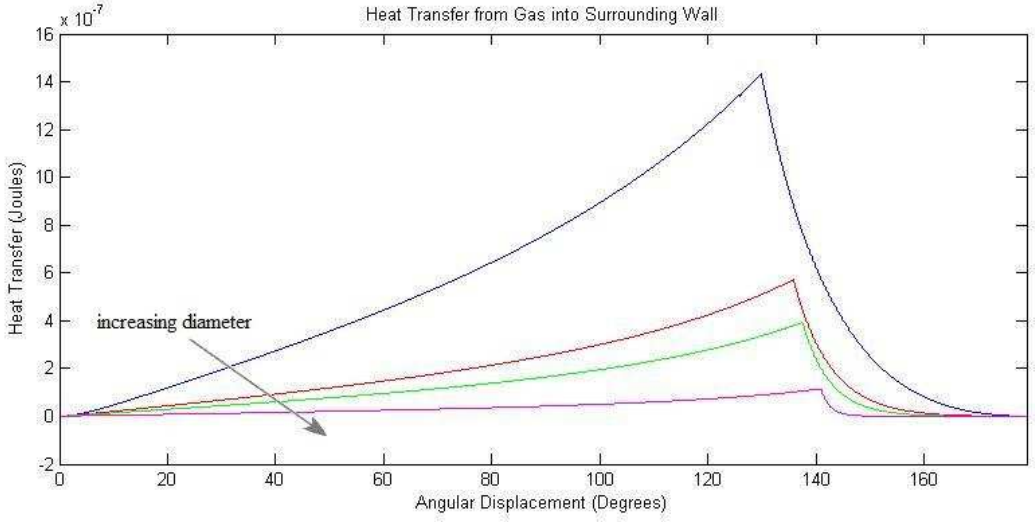

Figure 21: Variations in heat transfer from gas into surrounding wall at different bore diameters.

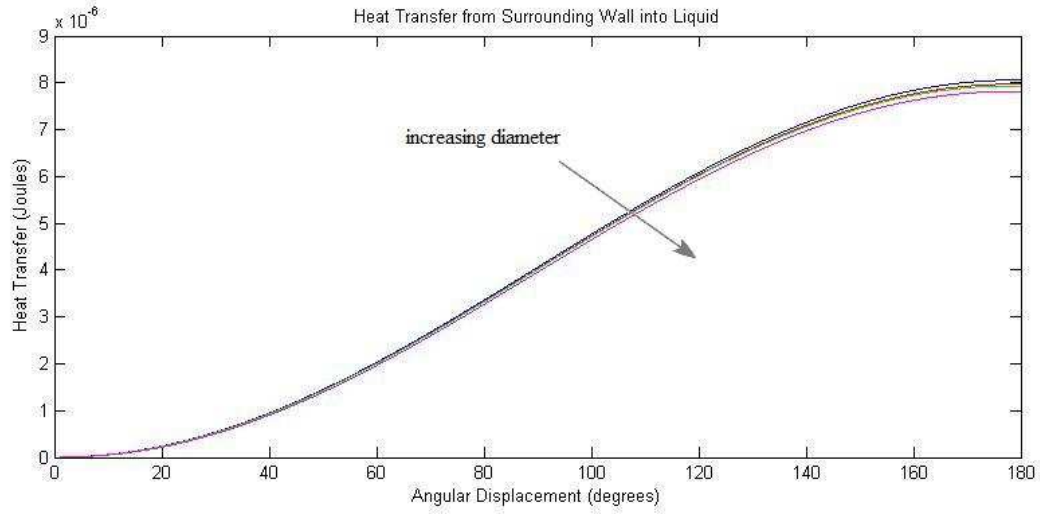

Figure 22: Variations in heat transfer from surrounding wall into liquid column at different bore diameters.

Helium-Water System

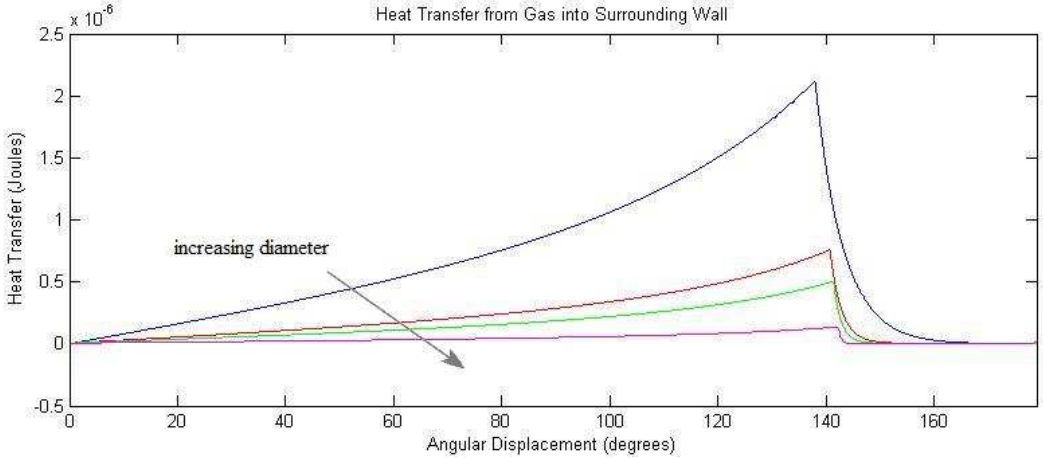

Figure 23: Variations in heat transfer from gas into surrounding wall at different bore diameters.

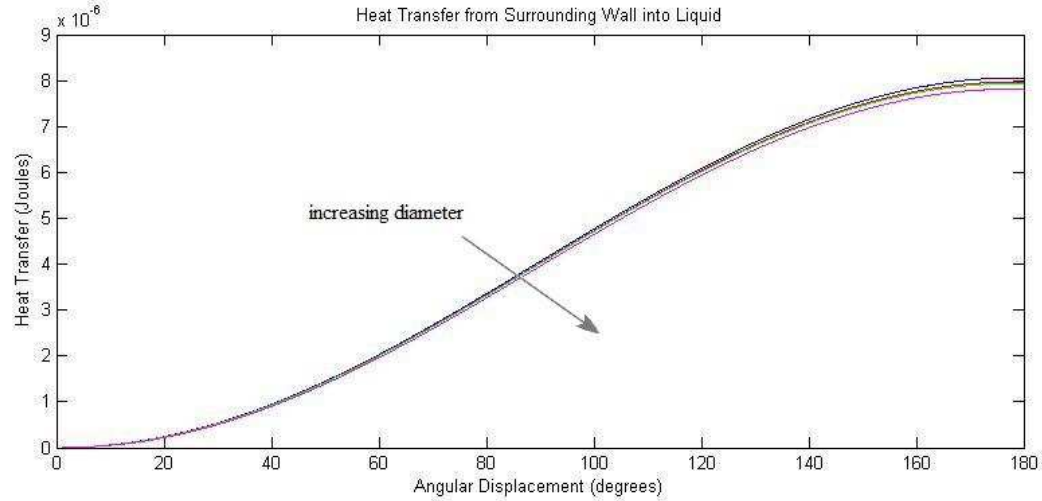

Figure 24: Variations in heat transfer from surrounding wall into liquid column at different bore diameters.

Air-DTE 25 System

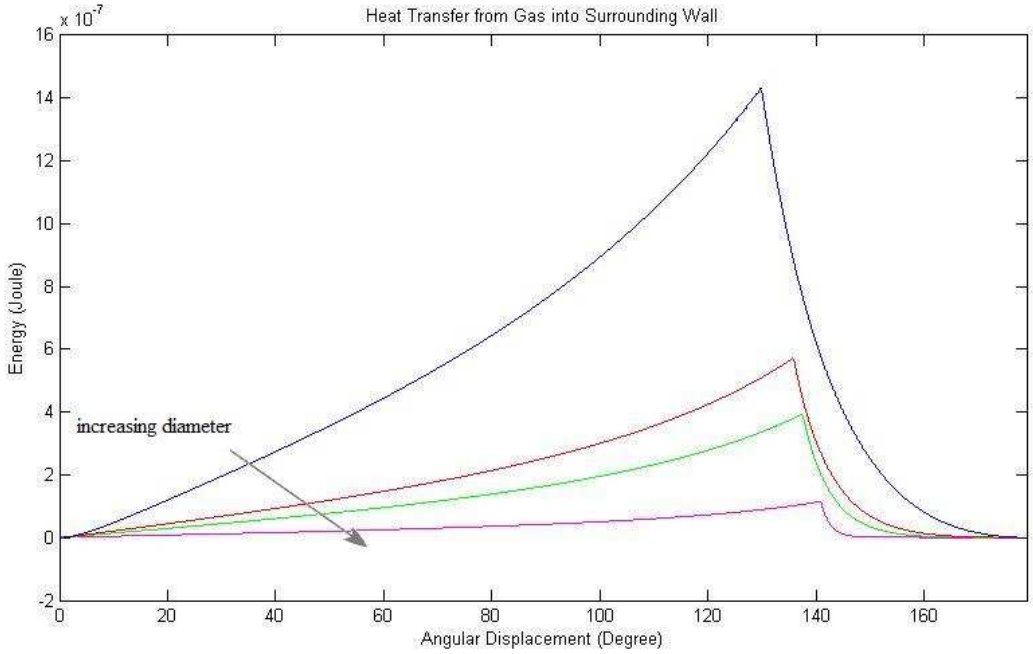

Figure 25: Variations in heat transfer from gas into surrounding wall at different bore diameters.

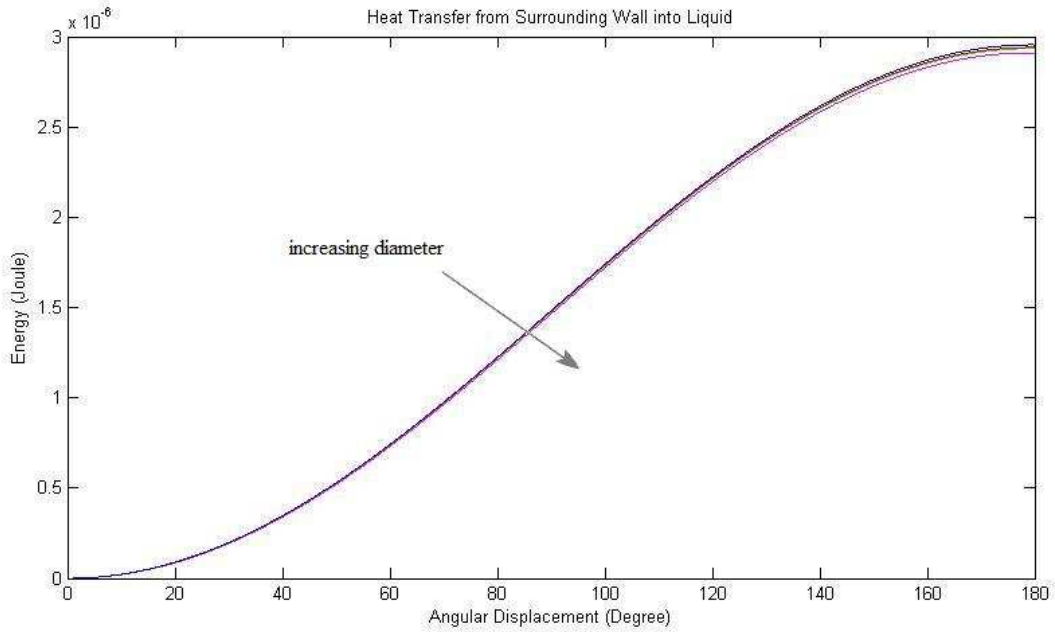

Figure 26: Variations in heat transfer from surrounding wall into liquid column at different bore diameters.

Helium – DTE 25 System

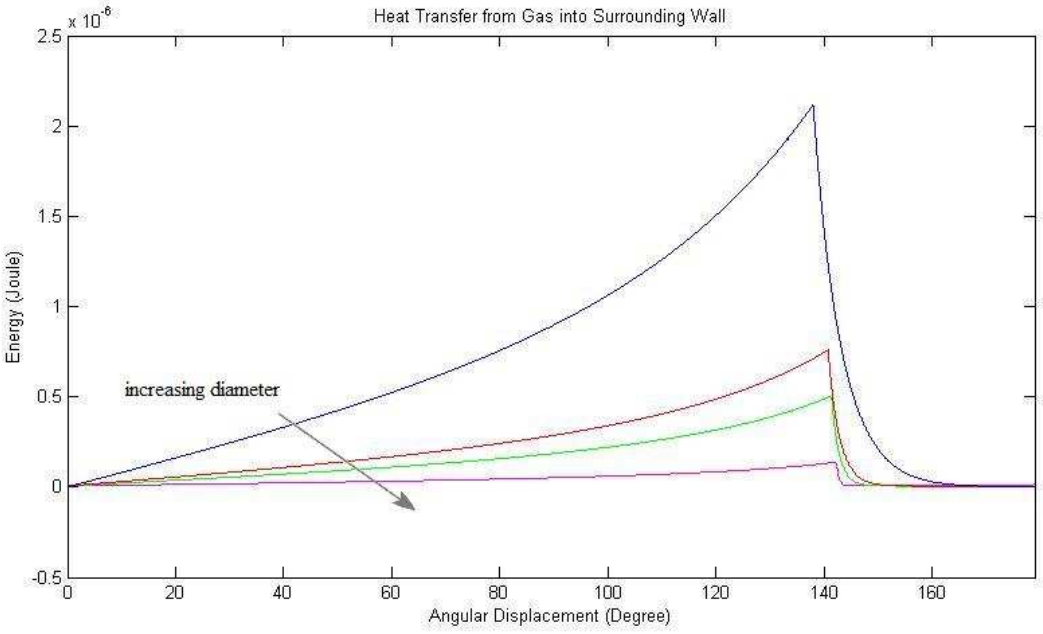

Figure 27: Variations in heat transfer from gas into surrounding wall at different bore diameters.

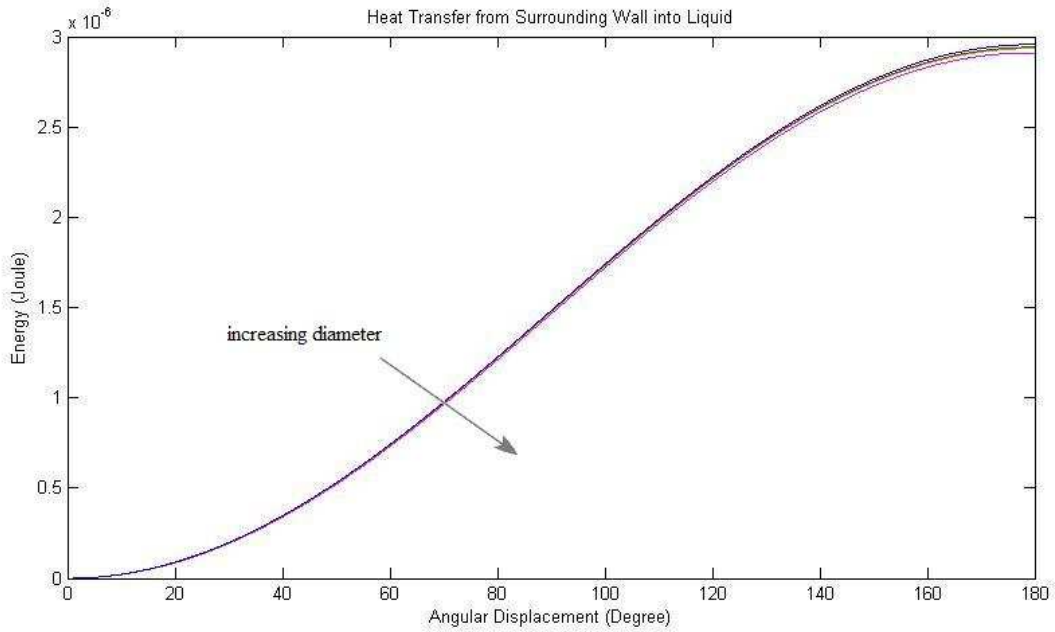

Figure 28: Variations in heat transfer from surrounding wall into liquid column at different bore diameters.

Impact of varying operation frequencies on radial heat transferred

The following plots show the radial heat transfer quantities to and from the surrounding walls while the bore diameter is kept constant at 0.9 mm. The frequencies are varied and the resulting heat transfer curves have been graphed against each other. The plots are categorized according the liquid piston and working gas combinations.

Figures 29, 31, 33 and 35 display the quantity of heat transfer occurring from the working gas to the surrounding bore wall. As before, the increasing gas temperatures induce an exponential increase in the heat transfer quantities. The figures identify that the radial heat transfer from the gas increases with decreasing operation frequencies. Unsurprisingly, the helium gas expels greater heat from itself to the bore walls in comparison to air.

Figures 30, 32, 34 and 36 display the quantity of radial heat transfer into the liquid column from the surrounding bore wall. As expected, the heat absorbed by the liquid column is also greater when operation frequencies are smaller. However, relatively the quantity of heat absorbed by water is greater than the quantity absorbed by DTE 25 at any operation frequency.

Air-Water System

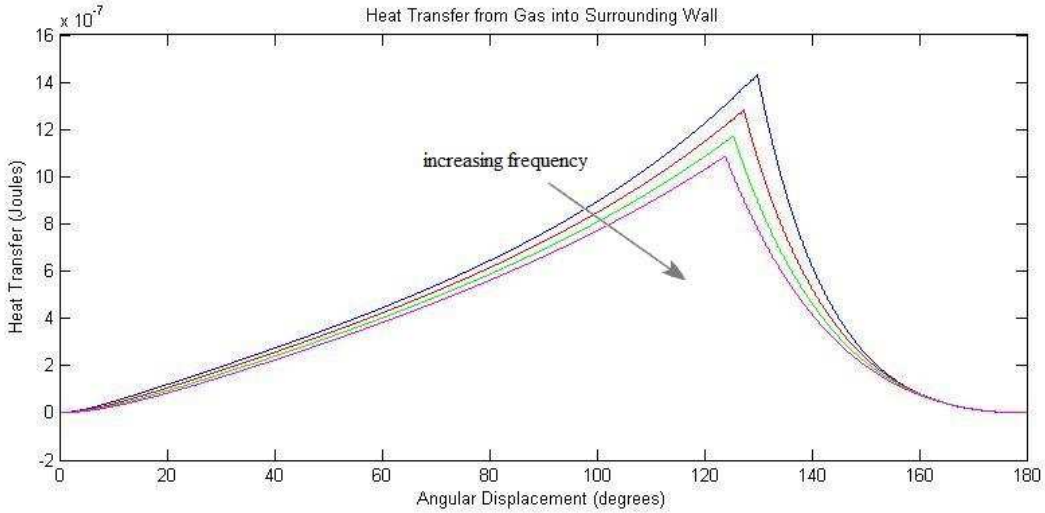

Figure 29: Variations in heat transfer from gas into surrounding wall at different frequencies.

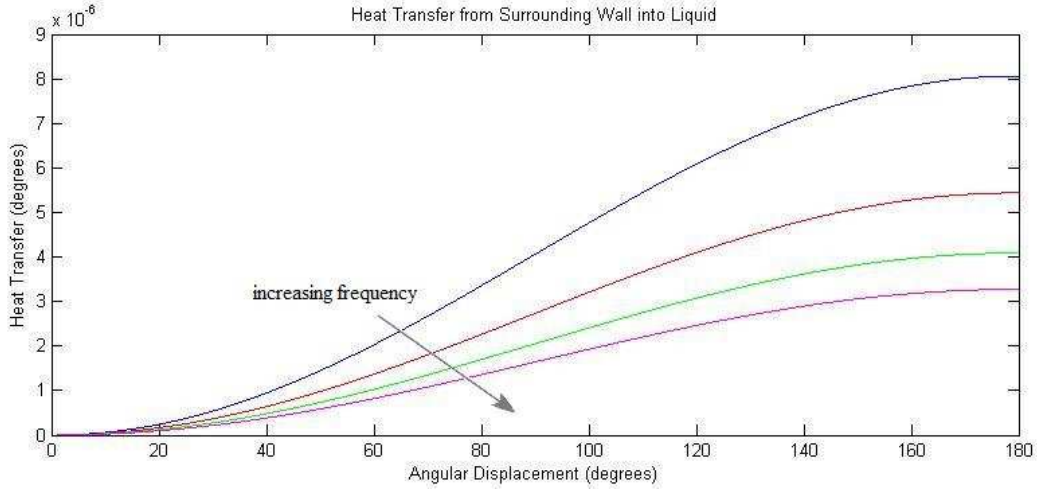

Figure 30: Variations in heat transfer from surrounding wall into liquid column at different frequencies.

Helium-Water System

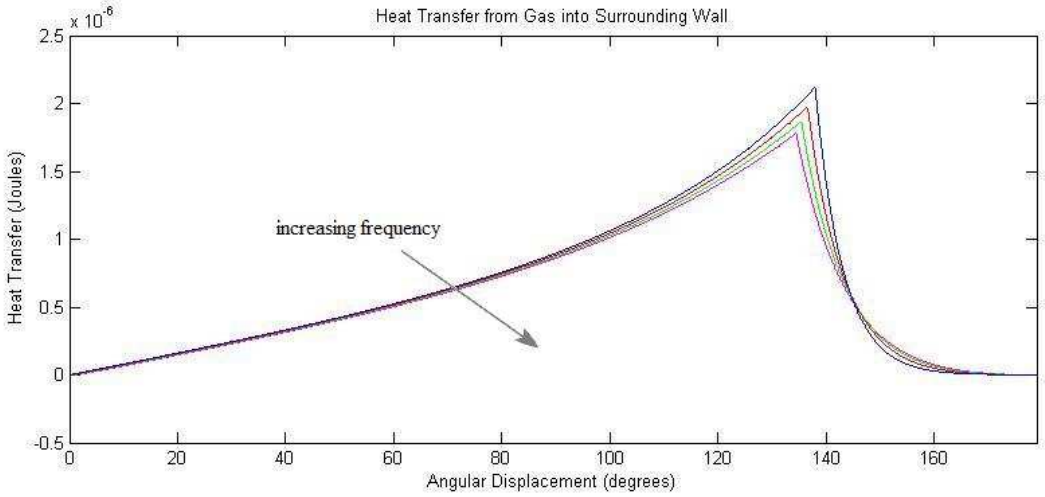

Figure 31: Variations in heat transfer from gas into surrounding wall at different frequencies.

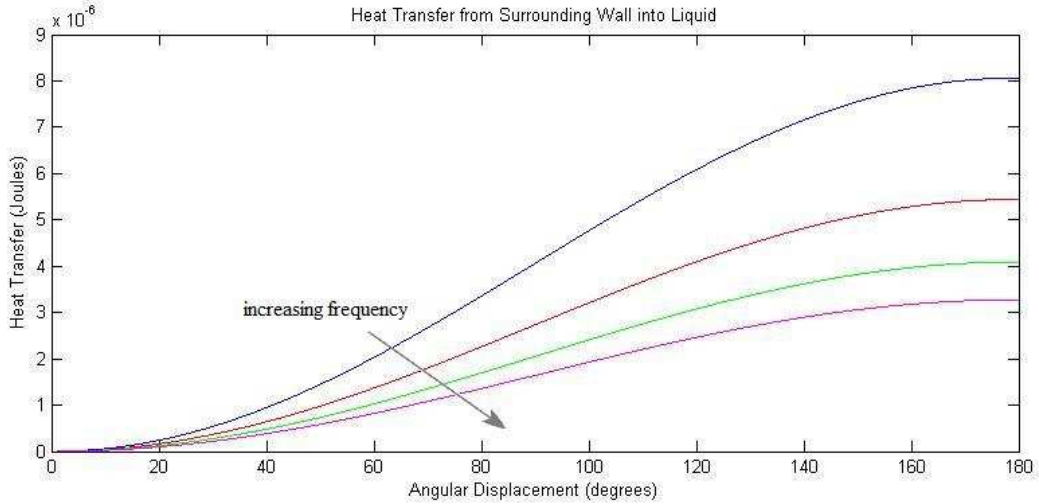

Figure 32: Variations in heat transfer from surrounding wall into liquid column at different frequencies.

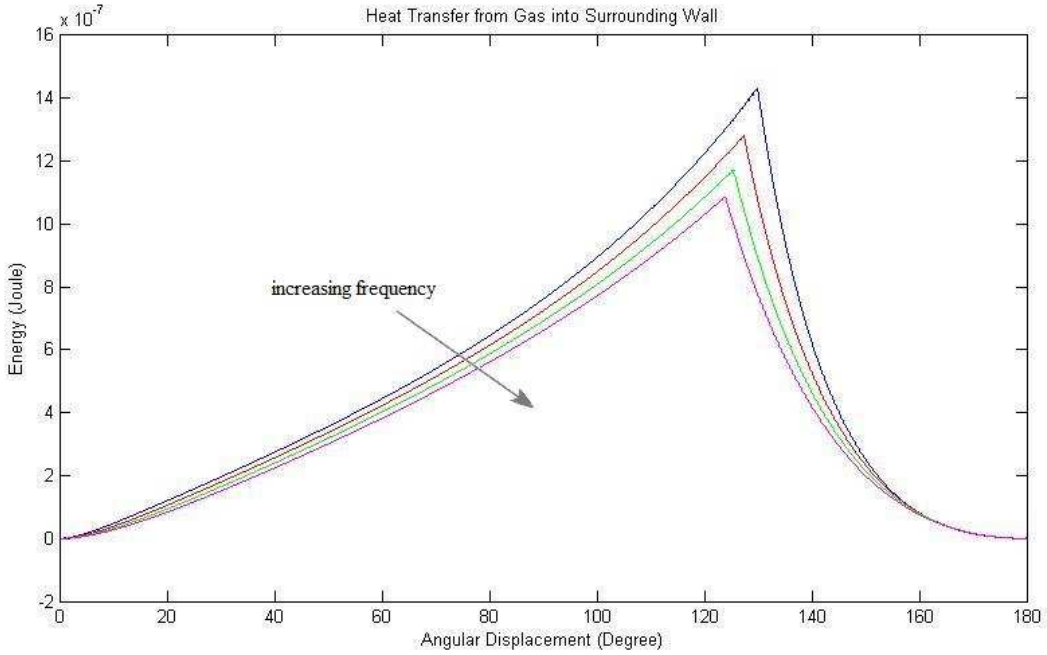

Figure 33: Variations in heat transfer from gas into surrounding wall at different frequencies.

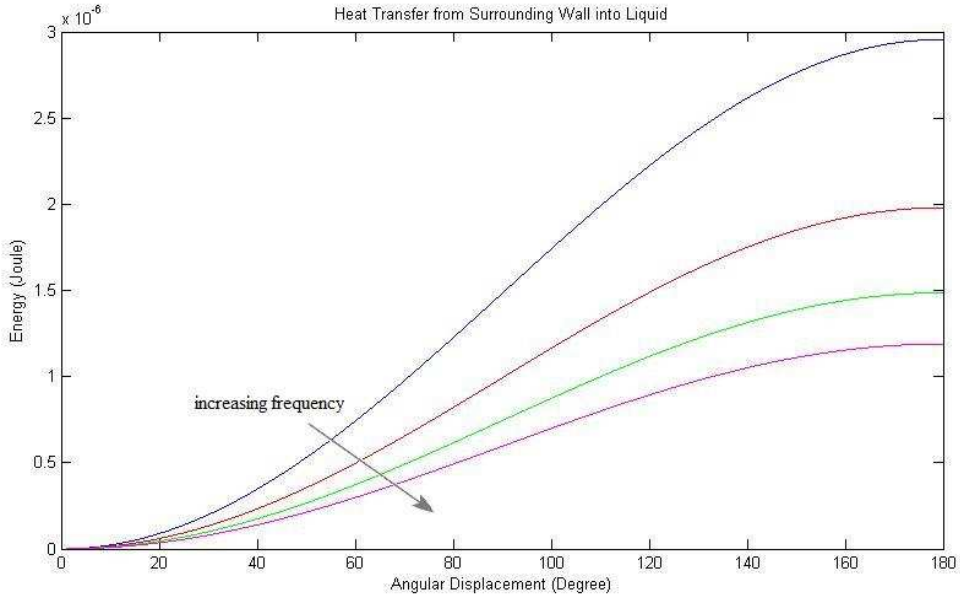

Figure 34: Variations in heat transfer from surrounding wall into liquid column at different frequencies.

Helium – Water System

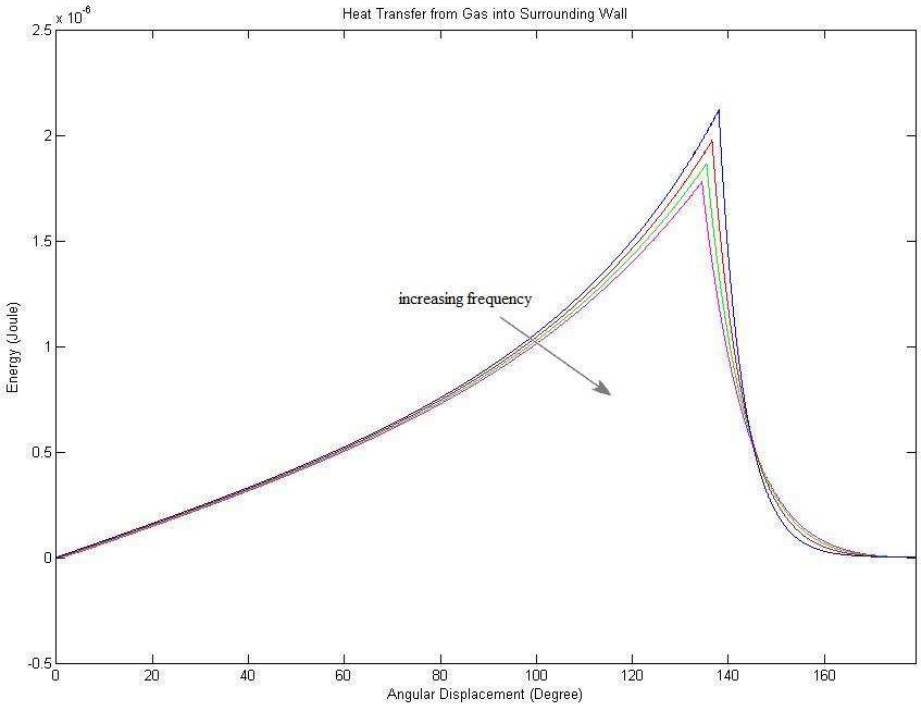

Figure 35: Variations in heat transfer from gas into surrounding wall at different frequencies.

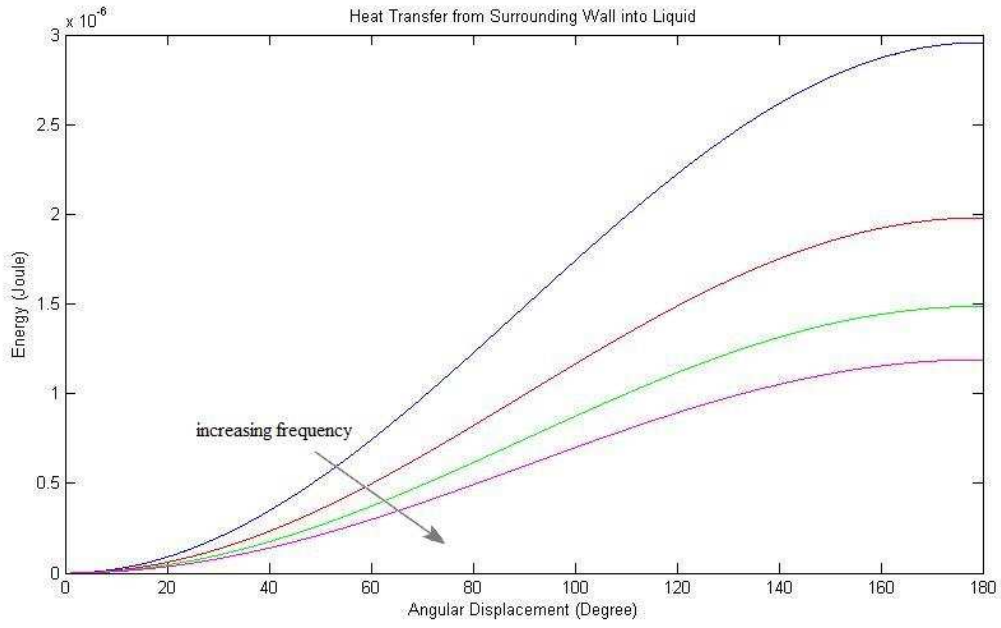

Figure 36: Variations in heat transfer from surrounding wall into liquid column at different frequencies.

Viscous Pressure Drops

To understand the contribution of the viscous forces due to the liquid column upon the over-all performance of the system, the instantaneous efficiency for the compression of the gas is graphed in Figure 37. The efficiency of compression is equated as the ratio of the work done to compress the gas to the total input energy. The curves are only equated for the regions in which compression occur. Therefore, the four curves end at slightly different points in the plot. The figure shows that the instantaneous efficiencies are very high and almost approach 100 %. Therefore, it can be concluded the viscous forces present in a single bore system are insignificant.

It is interesting to note that the efficiency curves do intersect each other at specific points. This implies that each system is not absolutely efficient for the entire compression stage and therefore we need to look at total efficiencies to compare the productiveness of each system. It is also interesting to note that for the most part, the DTE 25 systems are the least efficient due to the fluid's much higher viscosity in comparison to water close to room temperature.

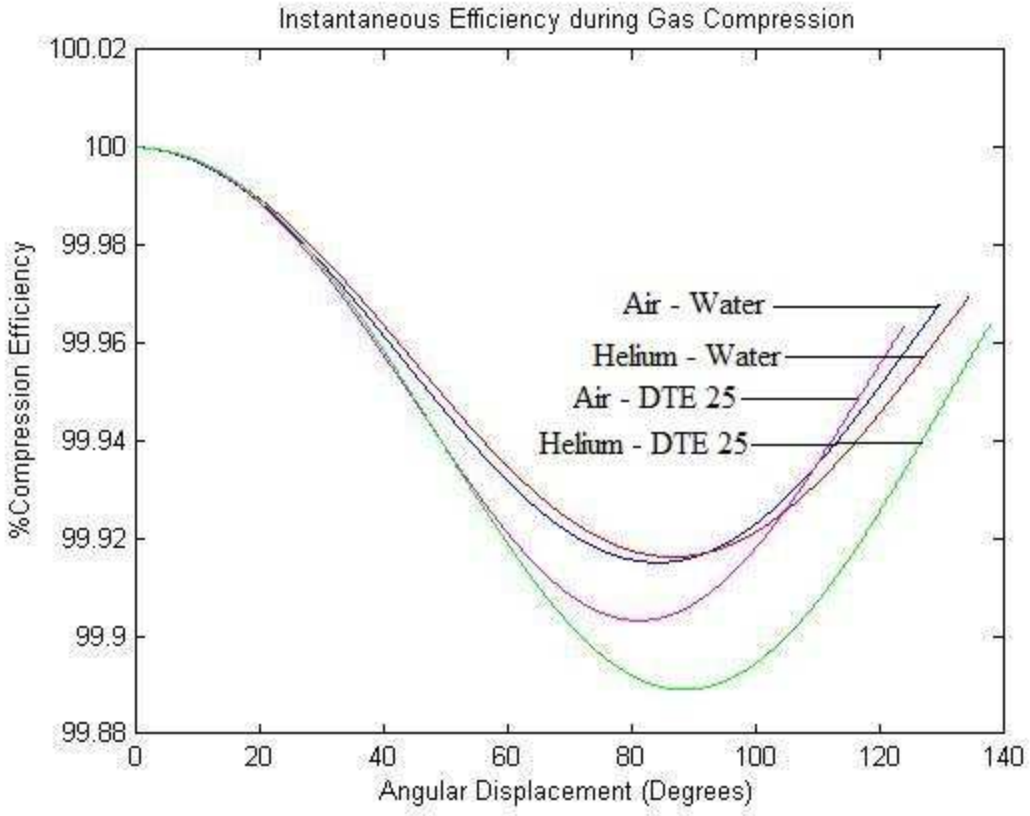

Figure 37: Instantaneous compression efficiencies for each system combination.

System Efficiency and Input Energy Quantities

Tables 7 and 8 contain two pieces of information for each system: 1) efficiency values and 2) input energy required to compress gas. Table 7 displays the efficiencies and input energies as the bore diameter is varied while Table 8 displays the efficiencies and input energies as the frequencies are varied.

Table 7: Efficiency and input energy of system relative to different bore diameters.

	Air and Water		Helium and Water		Air and DTE 25		Helium and DTE 25	
Diameters (mm) ↓	Eff (%)	Energy (Joules)	Eff (%)	Energy (Joules)	Eff (%)	Energy (Joules)	Eff (%)	Energy (Joules)
0.2	83.87	0.0066	87.71	0.0071	28.37	0.0195	31.16	0.02
0.4	86.88	0.0057	96.25	0.0063	83.95	0.0059	93.3	0.0065
0.5	82.75	0.0056	95.03	0.0062	82.01	0.0057	94.26	0.0063
0.9	66.53	0.0056	88.24	0.0061	66.52	0.0056	88.23	0.0061

Table 8: Efficiency and input energy of system relative to different frequencies of operation.

	Air and Water		Helium and Water		Air and DTE 25		Helium and DTE 25	
Frequencies (Hz) ↓	Eff (%)	Energy (Joules)	Eff (%)	Energy (Joules)	Eff (%)	Energy (Joules)	Eff (%)	Energy (Joules)
20	66.53	0.0056	88.24	0.0061	66.52	0.0056	88.23	0.0061
30	59.59	0.0056	84.94	0.0061	59.28	0.0056	84.47	0.0061
40	53.74	0.0056	81.34	0.0061	53.73	0.0056	81.34	0.0061
50	49.24	0.0056	78.61	0.0061	49.23	0.0056	78.61	0.0061

The maximum efficiency is achieved when the system is operating with a bore diameter of 0.4 mm in all cases except for the helium-DTE 25 combination. With respect to the operating frequency however, the maximum efficiencies are obtained at 20 Hz – the lowest operation frequency tested.

The highest absolute efficiency value of 96.25% is achieved using the helium and water system with a bore diameter of 0.4 mm and an operation frequency of 20 Hz.

The smallest energy value always occurs for the system with the largest bore diameter of 0.9 mm and a variation in diameter causes a relatively great change in the input energy values. However, no significant change in the quantity of input energy is noted when the frequencies are varied. The lower input energy required to compress the gas, 0.0056 joules, is constant for both air systems. The input energy required at the corresponding highest efficiency of 96.25% with respect to the bore diameter is 0.0063.

The next section will analyze the data to determine the physical explanations supporting them and attempt to identify the parameters for the optimum liquid piston compression system.

Analysis and Discussion

The goals of this project were to 1) construct a preliminary numerical model of a simplified liquid piston compression and 2) understand how system parameters could be varied to achieve optimum performance. As shown in the results, the main interest was in determining the effects of the bore diameter and the operation frequency upon the overall efficiency and input energy requirements of the system. In addition, the performance of helium and DTE 25 as the working gas and liquid piston respectively was evaluated against the baseline air-water system.

The gas temperature plots in Figures 13 through 16 clearly show that an increase in the bore diameter causes an increase in the gas temperatures during compression. This reaction is directly relevant to our principle motivation for creating a gas compression cylinder comprising of several thousand small diameter bores. Reduction of the bore diameters results in a greater metal surface area of contact between the working fluid and the system cylinder. In turn, a greater surface area of contact between the entire body of gas and the bore wall leads to an increase in the heat transfer from the gas. Similarly, a smaller diameter bore also increases the heat transfer between the bulk liquid column and the bore wall. This increase in the radial heat transfers to-and-from the wall is observed in the heat transfer plots (Figures 21 – 28).

Figures 17 through 20 display the effects on the gas temperatures as the frequency of operation is increased. A rise in the gas temperature is visible as the frequency of operation is increased. Heat transfer can be increased if the time of contact between the working gas and the wall is increased. However, an increase in the operation frequency reduces the time of contact between the gas and the bore wall essentially simulating an adiabatic system similar to a bicycle pump. In such a system, heat transfer from a gas is greatly reduced and the gas attains much higher temperatures as shown. Figures 29 through 36 support this theory; the graphs show that with increasing frequency of operation, heat transfer to-and-from the liquid is reduced.

Using just the gas temperatures and heat transfer plots, a conclusion about the most efficient system could not be reached. However, the tabulated efficiency and input energy values in Table 7 provide additional information that allow us to comprehend the trade-offs between efficiency and changes in diameter.

Firstly, it is seen that for most cases, the maximum efficiency occurs near 0.4 and 0.5 mm bore diameters. The variation in bore diameter is also seen to create a fluctuation in the input energy requirements of the system. Furthermore, the system comprising of the DTE 25 liquid piston consistently requires a greater quantity of input energy for compression than a system with water as the liquid piston.

These effects can be explained through two physical parameters of the fluids – dynamic viscosity and thermal conductivity. As identified previously in the paper, since the flow throughout the bore is

laminar, a strong viscous force between the liquid and the wall is expected. As the diameter of the bore is reduced, this viscous resistance is increased, resulting in a greater quantity of input energy expended to overcome it. Since water has a lower value of dynamic viscosity than DTE 25, the water column systems are more efficient.

Furthermore, water also has a greater capacity for absorbing energy due to its higher thermal conductivity. The property to absorb a greater quantity of heat allows the water column to cool the surrounding bore walls more efficiently. In turn, due to the interdependency between the heat transfers, the gas temperature is reduced and system efficiency for the water systems is increased.

The effects of varying the operation frequency are much more predictable. As expected, a lower frequency of operation results in a great efficiency due to the increase in the total time for radial heat transfers. However, hardly any fluctuations are noted in the input energy values as the frequencies are varied. Except for the observation that the water systems require lower input energies, the energy values remain quite similar for each case. Since the bore diameter is kept constant, this suggests that the majority of the input energy is expended to overcome the pressure forces exerted by the gas against the liquid column. As explained above, the water systems have lower input energy requirements because water has a greater capacity to absorb energy and therefore reduces the gas temperature more efficiently.

Another major observation from the graphs and tables is that helium – as the working gas – will provide a greater efficiency for the system than air. The gas temperatures are lowest and the gas to wall heat transfers is greatest when helium is used as the working gas instead of air. This is a result of helium's physical properties – mainly the higher specific heat constant and a higher thermal conductivity. The higher specific heat constant allows the gas to absorb greater energy with an increase in its temperature while the higher thermal conductivity allows the gas to transfer energy more readily.

Therefore, the results identify the most optimum liquid piston and working gas combination to be water and helium. The biggest discrepancy in the results occurs when comparing the bore diameter values where the maximum efficiency and the minimum input energy values are equated. The maximum efficiency for the helium and water system occurs for a bore diameter of 0.4 mm where as the lowest input energy needed for operating the system occurs at 0.9 mm. However, choosing the system according to the lowest input energy is not very rational since many of the inefficient modes require less energy than the helium and water system and would therefore be superior if judged only on that basis. If, for some reason a system was built to require less energy, then any of the less efficient modes would be suitable. On the other hand, in the interest of optimizing the efficiency of the system emphasis should be placed on the efficiency values more than the input energy values (all of which are relatively small anyways). Since that is our ultimate goal, this report concludes that for a single bore compression system, the most efficient and recommended mode of operation is at 20 Hz with a bore diameter of 0.4 mm using helium and water as the working gas and the liquid column respectively.

Recommendations for Future Study

The liquid piston gas compression model can be modified to resemble a more accurate system. The investigators involved in this study had identified additional physical phenomenon that would provide more accurate results when incorporated into the system. However, the team was unable to include these factors into the model due to a lack of time. The addition to the physical realism of the single bore system would include the viscous and heat transfer characteristics due to the boundary layer formation in laminar flows and the addition of a retraction cycle to produce a continuous oscillatory liquid piston engine instead of the currently existing single compression model.

Boundary Layer

Evaluating the heat transfer in a laminar flow through a single bore in the system can be further developed if the fluid properties are divided into two regions: one inside the boundary layer, which is the region adjacent to the surrounding bore walls where viscous forces are dominant, and the second throughout the remainder of the fluid. The boundary layer is formed due to the no-slip condition prevalent between the surrounding wall and the fluid adjacent to it. The boundary layer thickness is typically measured into the fluid from the surrounding wall up to the point where the fluid velocity is 99% of the bulk stream velocity. Within the bores of the liquid piston gas compressor a flat velocity gradient profile – as discussed in the section on *Radius Parameters*- causes this boundary layer to be very thin. However, it could still have significant effects on the radial heat transfer from the gas especially since the heat transfer quantities are so small.

The Reynolds number calculations for the liquid piston indicate that the flow will remain laminar throughout the entire compression cycle. This is an essential result since it allows the boundary layer to be represented as a thin layer of material of changing thickness enveloping the inner surface of the surrounding bore walls. This continuously varying boundary layer thickness, δ, can be evaluated using the following equation (Kreith and Bohn, 2000).

$$\delta = \mathrm{Re}^{-\frac{1}{2}} L = \sqrt{\frac{L\nu}{V}} \qquad \textbf{(E29.)}$$

L = length traveled by fluid
Re = Reynolds number
v = specific volume of fluid
V = velocity of column imparted by cam

Complete Oscillatory System

A complete oscillatory gas compression system comprising of a compression and retraction stage would produce much more accurate results since it is expected that over a period of operation, the system will assume a steady-state mode of operation – as an automobile engine does after operating for some time.

Evaluating the efficiency values at this instance would be more useful since the values will most probably approach the actual working efficiency of the system. Evaluating the efficiency for a single compression where the starting conditions are kept as standard room temperature conditions do not give us sufficient data about the continuous operation of the liquid piston compression engine.

However, an accurate representation of the liquid piston compression would require more advanced fluid dynamics modeling to account for any liquid surface instability such as splashing or liquid-gas interaction such as cavitation. Therefore, for modeling the oscillating compressor, using CFD software such as Fluent may be a better choice than MatLab.

Additional Parameters for Optimization

The results indicate that the bore sizes and the operating frequencies affect the performance of the system. However, several additional properties of this technology can be altered in an effort to maximize the efficiency.

1. Cylinder geometry

   Though the team did not have sufficient time to test complex cylinder geometries, surface area of contact between the working gas and the wall and the liquid piston and the wall can be increased if through the inclusion of surface features of through the use of unconventional shapes for the cylinder head. Some ideas are to include fins along the inner walls of the bores as seen in heat sinks or to alter the cylinder head to allow for an increase in the surface area (as using hemispherical or conical shapes).

2. Kinematic Parameters

   It is obvious that the kinematic parameter has a strong impact upon the heat-transfer characteristics of the liquid piston engine. Since the working gas in the bore attains greater temperatures as it is compressed further, a more optimum cam profile can be created that reduces the velocity of the liquid piston towards the upper regions of the cylinder to enable greater heat transfer from the gas to the wall and from the wall to the liquid. Ultimately, a cooler gas is easier to compress and would increase the efficiency and reduce the input power of the system.

Lastly, instead of concentrating on a single bore compression model, a complex multi-bore heat-transfer model will have to be created to evaluate the performance of the entire engine. After all, the ultimate goal of this project is to create a prototype working liquid piston engine. Such a detailed numerical model provides possibilities for experimentation and optimization without the need for prototypes. Thus, the numerical liquid piston engine model is a very powerful tool and will be useful to determine the parameters for the initial prototype. The results from this paper when combined with these possible improvements could ultimately produce a gas compression technology operating closer to an isothermal mode than any currently existing gas compression technology. With the current state of the global

energy supply, more efficient systems such as the liquid piston compression engine can make a large impact – especially considering all the areas in which gas compression technologies are utilized.

Bibliography

Norton, Robert L. *Design of Machinery*. 3rd ed. New York: McGraw-Hill Science, Engineering & Mathematics, 2003.

Kreith, Frank, and Mark Bohn. *Principles of Heat Transfer*. 6th ed. Boston: Course Technology, 2000.

Van de Ven, J. D., and Li, P. Y., "Liquid Piston Gas Compression," *Applied Energy-under review*, 2008.

Incropera, Frank P.Lavine, David P. DeWitt, and Theodore L. Bergman. *Fundamentals of Heat and Mass Transfer*. 6th ed. New York: John Wiley & Sons, Incorporated, 2006.

West, Colin D. *Liquid Piston Stirling Engine*. New York: John Wiley & Sons, Incorporated, 1983.

Fox, Robert W., Alan T. McDonald, and Philip J. Pritchard. *Introduction to Fluid Mechanics*. New York: John Wiley & Sons, Incorporated, 2005.

Zamir, M., and E. L. Ritman. *The Physics of Pulsatile Flow*. Ed. E. Greenbau. New York: Springer, 2000.

Cengel, Yunus A., and Michael A. Boles. *Thermodynamics*. 6th ed. New York: McGraw-Hill Companies, 2001.

Brennen, Christopher E. *Cavitation and Bubble Dynamics*. USA: Oxford University, 1995.

"Mobil DTE 20 Series." MOBIL. 01 Feb. 2009 <http://www.mobil.com/Canada-English/Lubes/PDS/IOCAENINDMOMobil_DTE_20_Series.asp>.

Engineering ToolBox. 01 Feb. 2009 <http://www.engineeringtoolbox.com>.

Appendix

Matlab Code

The code formatting is appropriate for copy and pasting onto Matlab directly. This particular code pertains to the air-water system. To accommodate other combinations, the physical constants have to be changed accordingly.

```
%-----------------------------------------------------
clear;  clc;
%defining constants for specific heat constant of air
%-----------------------------------------------------
a = 28.11;
b = 0.1976*10^-2;
c = 0.4802*10^-5;
e = -1.966*10^-9;
%-----------------------------------------------------

%defining kinematic parameters
%-------------------------------------------
freq = 20;                          %liquid piston operating frequency
w = 2*pi*freq;                      %angular velocity of cam-follower
d = 0.0009;                         %individual bore diameter
h = 0.0393;                         %stroke length
timestep = 9500;                    %number of compression time period divisions
deltat= (1/(2*freq))/timestep;      %value of individual compression time
                                     increment
divisor = 9500;                     %number of stroke length increments
deltaY = (h/divisor);               %incremental displacement of liquid piston

%-------------------------------------------

%defining initial/boundary conditions
%-------------------------------------------
T(1) = 298;                         %initial temperature
P(1) = 101300;                      %initial pressure of 1 atm
M = 1.2*h*pi*(d/2)^2;               %total mass of working gas calculated at sea-
                                     level using density of 1.2kg/m^3
%-------------------------------------------

%defining geometrical parameters
%-------------------------------------------
Across = pi*(d/2)^2;                %cross-sectional area of bore
Steelden=7850;                      %density of steel
t = .000488;                        %bore wall thickness
Asl = deltaY*pi*d;                  %inner bore wall surface area for each
                                     differential volume
Mring = (pi*((((d/2)+t)^2)-((d/2)^2)))*deltaY*Steelden; %mass of inner bore
                                                         wall differential
                                                         volume
Aaxial = (pi*((((d/2)+t)^2)-((d/2)^2)));    %radial cross sectional surface
```

```
                                                area of bore
kliquid = .58;                  %conductive coefficient for liquid piston
visliq = 1.155*(10^-3);         %viscosity of liquid piston
liqden = 1000;                  %density of liquid piston
%-----------------------------------------

%defining heat transfer parameters
%-----------------------------------------
kst = 25;                       %conductive coefficient of surrounding wall
hg = 4.36*.025/d;               %convective coefficient of working gas
ha = 50;                        %convective coefficient of surroundings
hl = 4.36*kliquid/d;            %convective coefficient of liquid piston
R = 287;                        %ideal gas constant for working gas
Cpst = 500;                     %specific heat capacity of surrounding wall
Tl = 288;                       %constant temperature of liquid piston
%-----------------------------------------

%defining operational variables
%---------------------------------
Tm = ones(timestep,divisor);    %instantaneous metal temperature
Tinitial = 298;                 %initial working gas temperature
Tbulk = 298;
P(timestep) = 0;                %instantaneous working gas pressure
Qin(divisor) = 0;               %axial heat transfer into a single bore wall
                                 differential volume
Qout(divisor) = 0;              %axial heat transfer out of a single bore
                                 wall differential volume
tracker=0;                      %variable to track critical pressure point
Pressure = 0;
Density = 0;
Tg(timestep) = 0;               %instantaneous working gas temperature
E(timestep) = 0;                %instantaneous input energy
Etotal = 0;                     %total input energy during compression
Eviscous(timestep) = 0;         %instantaneous energy consumed by viscous
                                 forces
Eviscoustotal = 0;              %total energy consumed by viscous forces
Epressure(timestep) = 0;        %instantaneous energy consumed by pressure
                                 forces
Epressuretotal = 0;             %total energy consumed by pressure forces
temp(timestep) = 0;
Pliquid(timestep) = 0;          %instantaneous pressure exerted by the liquid
                                 piston
Pliqviscous(timestep) = 0;      %instantaneous pressure loss due to viscosity
                                 in liquid pistons
W = 0;
Qgas(timestep) = 0;             %instantaneous radial heat transfer from gas
Qliq(timestep) = 0;             %instantaneous radial heat transfer into
                                 liquid piston
num(timestep)=0;
den(timestep)=0;
%---------------------------------

%determining instantaneous kinematic and physical properties
%-------------------------------------------------------------
for i = 1:timestep
```

```
    time(i) = deltat * i;                %time instance
    s(i) = (h/2)*(1-cos(w*time(i)));     %instantaneous displacement
    v(i) = (h/2)*(sin(w*time(i)));       %instantaneous velocity
    Abulk(i) = (h-s(i))*(pi*d);          %instantaneous surface area of
                                          contact between bore wall and
                                          working gas
    Mbulk(i) = (pi*((((d/2)+t)^2)-((d/2)^2)))*(h-s(i))*Steelden;
    %instantaneous mass of bore wall in contact with working gas
end
%-------------------------------------------------------------------

%determining instantaneous thermal fluid parameters during compression
%-------------------------------------------------------------------------
for i = 1:timestep
    %specifying specific heat values
    %---------------------------------
    if i == 1
        Cp = (a+b*Tinitial+c*Tinitial^2+e*Tinitial^3);
    else
        Cp = (a+b*Tg(i-1)+c*Tg(i-1)^2+e*Tg(i-1)^3);
    end

    Cv = R - Cp;
    %---------------------------------

    %correlating time steps with piston displacement
    %-----------------------------------------------
    counter = 0;
    while (counter*deltaY < s(i))
        counter = counter+1;
    end
    %-----------------------------------------------

    %determining instantaneous temperature and input work
    %---------------------------------------------------
    if i == 1
        Tg(i) = ((M*Cv*298)-(1/2)*(M*((v(i))^2)) +
hg*Abulk(i)*Tbulk*deltat)/((M*Cv)+(hg*Abulk(i)*deltat)+(M*R*(0-s(i))/(h-
s(i))));
        Work(i)= (M*R*Tg(i)*(0-s(i))/(h-s(i)));
        W = W + (M*R*Tg(i)*(0-s(i))/(h-s(i)));
    else
        Tbulk = 0;
        for j = (counter):divisor
            Tbulk = Tbulk + Tm(i-1,j);
        end
        Tg(i) = ((hg*Asl*deltat*Tbulk)+(M*Cv*Tg(i-1))-(0.5*M*((v(i)^2)-((v(i-
1)^2)))))/((M*Cv)+(hg*Asl*deltat*(divisor-counter))+(M*R*(s(i-1)-s(i))/(h-
s(i))));
        Work(i) = (M*R*Tg(i)*(s(i-1)-s(i))/(h-s(i)));
        W = W + (M*R*Tg(i)*(s(i-1)-s(i))/(h-s(i)));
    end
    %-----------------------------------------------------
```

```
%determining instantaneous radial heat transfer values
%-------------------------------------------------------
if i == 1
    Qbulk = hg*Abulk(i)*deltat*(Tg(i)-Tbulk);
    Qgas(i) = Qbulk;
    Tbulk = (Qbulk/(Mbulk(i)*Cpst))+Tbulk;
    temp(i) = Tbulk;
end

if i == 1
    for j = (counter):divisor
        Tm(i,j)=Tbulk;
    end
else
    for j = counter:divisor
        Q = hg*Asl*deltat*(Tm(i-1,j)-Tg(i));
        Qgas(i) = Qgas(i)+ Q;
        Tm(i,j)=Tm(i-1,j)-(Q/(Mring*Cpst));
    end

end

if i > 1
    for j = 1:counter-1
        if Tm(i-1,j) > 1
            if Tl < Tm(i-1,j)
                Ql = hl*Asl*deltat*(Tl-Tm(i-1,j));
                Qliq(i) = Qliq(i) + Ql;
                Tm(i,j) = (Ql/(Mring*Cpst))+Tm(i-1,j);
            end
        end
    end
end
%-------------------------------------------------------

%determining instantaneous axial heat transfer values
%----------------------------------------------------
for j = 1:divisor
    if j == 1
        if Tl < Tm(i,j)
            Qout(j) = hl*Aaxial*deltat*(Tl-Tm(i,j));
        end
        if Tm(i,j+1) > Tm(i,j)
            Qin(j) = (kst*Aaxial*deltat*(Tm(i,j+1)-Tm(i,j)))/deltaY;
        end
    else
        Qout(j) = -Qin(j-1);
        if j < divisor
            if Tm(i,j+1) > Tm(i,j)
                Qin(j) = (kst*Aaxial*deltat*(Tm(i,j+1)-Tm(i,j)))/deltaY;
            end
        else
            Qin(j) = 0;
        end
    end
```

```
        Qtotal(j) = Qin(j) + Qout(j);
        if Qtotal(j)<0
         Tm(i,j) = (Qtotal(j)/(Mring*Cpst))+Tm(i,j);
        end
    end
    %-------------------------------------------------------

    %determining instantaneous working gas pressure and system efficiency
    %-----------------------------------------------------------------------
    P(i)=(M/(Across*(h-s(i))))*R*Tg(i);

    if i > 1
        E(i) =
((P(i)*Across)+(liqden*Across*s(i)*9.81)+(pi*d*s(i)*(visliq)*v(i)/(d/2)))*(s(
i)-s(i-1));
        Eviscous(i) = (pi*d*s(i)*(visliq)*v(i)/(d/2))*(s(i)-s(i-1));
        Epressure(i) = (P(i)*Across)*(s(i)-s(i-1));
    else
        E(i) =
((P(i)*Across)+(liqden*Across*s(i)*9.81)+(pi*d*s(i)*(visliq)*v(i)/(d/2)))*(s(
i));
        Eviscous(i) = (pi*d*s(i)*(visliq)*v(i)/(d/2))*(s(i));
        Epressure(i) = (P(i)*Across)*(s(i));
    end

    Etotal = Etotal + E(i);
    Eviscoustotal = Eviscoustotal + Eviscous(i);
    Epressuretotal = Epressuretotal + Epressure(i);

    temp(i)=M;

    Pliquid(i) = ((8*visliq*s(i)*Across*v(i))/(pi*((d/2)^4))) + P(i) +
liqden*(s(i))*(9.81);
    Pliqviscous(i) = ((8*visliq*s(i)*Across*v(i))/(pi*((d/2)^4)));

    Efficiency(i) = (-Work(i)/E(i))*100;
    Efficiency2(i) = (Qgas(i)/E(i))*100;
    x(i)=Pliqviscous(i)/Pliquid(i);
    %-----------------------------------------------------------------

    %checking pressure ratio and terminating compression
    %-------------------------------------------------------
    if ((P(i)/P(1))>=9.8)
        tracker = i;
        Pressure = P(i);
        Eff = W/Etotal;
        break;
    end
    %-----------------------------------------------------------------------
end

result(timestep)=0;

%determining instantaneous thermal fluid parameters during gas expulsion
```

```
%-------------------------------------------------------------------------
for i = (tracker+1):timestep
    %specifying specific heat values
    %--------------------------------
    Cp = (a+b*Tg(i-1)+c*Tg(i-1)^2+e*Tg(i-1)^3);
    Cv = R - Cp;
    %--------------------------------

    %correlating time steps with piston displacement
    %-----------------------------------------------
    counter = 0;
    while (counter*deltaY < s(i))
        counter = counter+1;
    end
    %-----------------------------------------------

    %determining instantaneous temperature and input work
    %---------------------------------------------------
    Density = Pressure/(R*Tg(i-1));
    M = Across*(h-s(i-1))*Density;
    deltaM = -M + Across*(h-s(i-2))*Density;
    temp(i)=M;
    Tbulk = 0;
    for j = (counter):divisor
        Tbulk = Tbulk + Tm(i-1,j);
    end
    Tg(i) = ((hg*Asl*deltat*Tbulk)+(M*Cv*Tg(i-1))-(0.5*M*((v(i)^2)-((v(i-
1)^2)))))/((M*Cv)+(hg*Asl*deltat*(divisor-counter)));
    num(i) = (hg*Asl*deltat*Tbulk);
    den(i) = (M*Cv)+(hg*Asl*deltat*(divisor-counter));
    result(i)=num(i)/den(i);
    %---------------------------------------------------

    %determining instantaneous radial heat transfer values
    %-----------------------------------------------------
    for j = counter:divisor
        Q = hg*Asl*deltat*(Tm(i-1,j)-Tg(i));
        Tm(i,j)=Tm(i-1,j)-(Q/(Mring*Cpst));
        Qgas(i) = Qgas(i)- Q;
    end

    if i > 1
    for j = 1:counter-1
        if Tm(i-1,j) > 1
            if Tl < Tm(i-1,j)
                Ql = hl*Asl*deltat*(Tl-Tm(i-1,j));
                Qliq(i) = Qliq(i)+ Ql;
                Tm(i,j) = (Ql/(Mring*Cpst))+Tm(i-1,j);
            end
        end
    end
    end

    %-----------------------------------------------------
```

```
    %determining instantaneous axial heat transfer values
    %-----------------------------------------------------
    for j = 1:divisor
        if j == 1
            if Tl < Tm(i,j)
                Qout(j) = hl*Aaxial*deltat*(Tl-Tm(i,j));
            end
            if Tm(i,j+1) > Tm(i,j)
                Qin(j) = (kst*Aaxial*deltat*(Tm(i,j+1)-Tm(i,j)))/deltaY;
            end
        else
            Qout(j) = -Qin(j-1);
            if j < divisor
                if Tm(i,j+1) > Tm(i,j)
                    Qin(j) = (kst*Aaxial*deltat*(Tm(i,j+1)-Tm(i,j)))/deltaY;
                end
            else
                Qin(j) = 0;
            end
        end
        Qtotal(j) = Qin(j) + Qout(j);
        if Qtotal(j)<0
         Tm(i,j) = (Qtotal(j)/(Mring*Cpst))+Tm(i,j);
        end
    end
    %-----------------------------------------------------

    %determining system efficiency
    %-----------------------------------------------------------------------
    E(i) =
((P(i)*Across)+(liqden*Across*s(i)*9.81)+(pi*d*s(i)*(visliq)*v(i)/(d/2)))*(s(
i)-s(i-1));
    Eviscous(i) = (pi*d*s(i)*(visliq)*v(i)/(d/2))*(s(i)-s(i-1));
    Epressure(i) = (P(i)*Across)*(s(i)-s(i-1));


    Etotal = Etotal + E(i);
    Eviscoustotal = Eviscoustotal + Eviscous(i);
    Epressuretotal = Epressuretotal + Epressure(i);

    Pliquid(i) = ((8*visliq*s(i)*Across*v(i))/(pi*((d/2)^4))) + Pressure +
liqden*(s(i))*(9.81);
    Pliqviscous(i) = ((8*visliq*s(i)*Across*v(i))/(pi*((d/2)^4)));
    %-----------------------------------------------------------------------
end

%determining final efficiencies
%------------------------------
for i = 1:tracker
    Qgas(i)=-1*Qgas(i);
    Efficiency2(i)=-1*Efficiency2(i);
end
```

```
for i = 1:timestep
    Qliq(i)=-1*Qliq(i);
end

Vfinal = (Across * (h-s(tracker)))*298/Tg(tracker);
Workloss = Pressure*(Vfinal - (Across * (h-s(tracker))));
Finalenergy = W - Workloss;
Finaleff = Finalenergy/Etotal;
%---------------------------------------
```